Chapter | five

Linear Equations of Relative Motion

It is the mark of an educated mind
to rest satisfied with the degree of precision
which the nature of the subject admits
and not to seek exactness
where only an approximation is possible.

Aristotle (384 BC–322 BC)

In this chapter, we present a variety of linear differential equations for modeling relative motion under the two-body assumptions. The systems of equations for the description of relative motion can be classified according to the coordinate system utilized – Cartesian or curvilinear. There are also the issues of the choices of the independent variable – time or an angle variable and the space in which the linearization is carried out, e.g., physical coordinates vs. a set of orbital elements. The focus in this chapter is on the physical coordinate description of relative motion; motion description by the orbital elements is treated extensively in Chapter 6. This chapter begins with a discussion of the derivation of the linearized equations of relative motion with respect to a circular reference orbit, also known as the Clohessey–Wiltshire (CW) equations [101]. The CW equations have found extensive use for the analysis, design, and control of formations and a brief description of these applications is given in Section 5.2. Section 5.3 presents a derivation of the CW equations from the perspective of analytical mechanics, via the Lagrangian and the Hamiltonian. Section 5.5 presents a comparison and error analysis of the linearized equations obtained by using Cartesian and curvilinear coordinates. This section is followed by the presentation of the Tschauner–Hempel equations [102] for elliptic reference orbits. Brief descriptions of several approaches to the derivation of the two-body relative motion State Transition Matrix (STM) are also included. The chapter ends with a discussion of the application of the elliptic reference orbit STM to obtain initial conditions for preventing secular drift and alternatively, for the computation of impulsive maneuvers for establishing or initializing formations.

Spacecraft Formation Flying; ISBN: 9780750685337

5.1 THE CLOHESSY–WILTSHIRE EQUATIONS

In Section 4.5 we developed the nonlinear equations of relative motion assuming that the chief's orbit is circular. This simplification rendered an autonomous set of nonlinear differential equations. If the deputy's orbit in the inertial space is only slightly elliptic and slightly inclined with respect to the chief's orbit, the motion of the deputy will appear very close to the chief in a chief-fixed frame, provided that the initial positions are first-order small. In this case, Eqs. (4.74)–(4.76) may be linearized about the origin of the chief-fixed frame, $\mathscr{L}$, and the resulting motion may be solved in closed-form. The linearized equations of motion are called the *Clohessy–Wiltshire equations* (CW) or the *Hill–Clohessy–Wiltshire equations* (HCW).[1] These equations were developed by CW in the early 1960s to analyze spacecraft rendezvous [101].

There are a number of ways to develop and solve the CW equations. We will discuss some of these methods, as each method contributes insight into the relative motion problem.

A straightforward approach for developing the CW equations is to expand the right-hand side of Eqs. (4.74)–(4.76) into a Taylor series about the origin. Taking only the first-order terms and denoting $n_0 = \sqrt{\mu/a_0^3}$ we get

$$-\frac{\mu(a_0+x)}{\left[(a_0+x)^2+y^2+z^2\right]^{\frac{3}{2}}} \approx n_0^2(2x-a_0) \tag{5.1}$$

$$-\frac{\mu y}{\left[(a_0+x)^2+y^2+z^2\right]^{\frac{3}{2}}} \approx -n_0^2 y \tag{5.2}$$

$$-\frac{\mu z}{\left[(a_0+x)^2+y^2+z^2\right]^{\frac{3}{2}}} \approx -n_0^2 z \tag{5.3}$$

Rearranging and omitting the subscript 0 (so that $n \equiv n_0$ and $a \equiv a_0$) yields

$$\ddot{x} - 2n\dot{y} - 3n^2 x = 0 \tag{5.4}$$

$$\ddot{y} + 2n\dot{x} = 0 \tag{5.5}$$

$$\ddot{z} + n^2 z = 0 \tag{5.6}$$

Equations (5.4)–(5.6) are the CW equations with no disturbing and/or control accelerations. The nonhomogeneous forms of Eqs. (5.4)–(5.6) are

$$\ddot{x} - 2n\dot{y} - 3n^2 x = d_x + u_x \tag{5.7}$$

$$\ddot{y} + 2n\dot{x} = d_y + u_y \tag{5.8}$$

$$\ddot{z} + n^2 z = d_z + u_z \tag{5.9}$$

[1] These equations are sometimes referred to as *Hill's equations*, as Hill was the first to develop linearized relative equations of motion to describe the Moon's orbit in a rotating Earth-centric frame. However, we will avoid using the term "Hill's equations" because in mathematics this term is reserved for the equation $\frac{\mathrm{d}^2 y}{\mathrm{d}x^2} + \left(\theta_0 + 2\sum_{n=1}^{\infty}\theta_n \cos(2nx)\right) y = 0$, where the θ's are constants.

where $[d_x, d_y, d_z]^T$ and $[u_x, u_y, u_z]^T$ are, respectively, the vectors of environmental perturbations and control accelerations. One often normalizes the relative coordinates by the radius of the reference orbit, a, and the angular velocities by n, so that in normalized form the unforced CW equations (5.4)–(5.6) become

$$\bar{x}'' - 2\bar{y}' - 3\bar{x} = 0 \tag{5.10}$$

$$\bar{y}'' + 2\bar{x}' = 0 \tag{5.11}$$

$$\bar{z}'' + \bar{z} = 0 \tag{5.12}$$

where $(\cdot)'$ denotes differentiation with respect to normalized time. It is convenient to write the linear differential equations (5.4)–(5.6) in state-space form. Choosing the state vector $\mathbf{x} = [x, y, z, \dot{x}, \dot{y}, \dot{z}]^T$, Eqs. (5.4)–(5.6) assume the form

$$\dot{\mathbf{x}}(t) = A\mathbf{x}(t) \tag{5.13}$$

where A is the *system matrix*, given by

$$A = \begin{bmatrix} 0 & 0 & 0 & 1 & 0 & 0 \\ 0 & 0 & 0 & 0 & 1 & 0 \\ 0 & 0 & 0 & 0 & 0 & 1 \\ 3n^2 & 0 & 0 & 0 & 2n & 0 \\ 0 & 0 & 0 & -2n & 0 & 0 \\ 0 & 0 & -n^2 & 0 & 0 & 0 \end{bmatrix}, \tag{5.14}$$

and the initial conditions are $\mathbf{x}(t_0) = [x(t_0), y(t_0), z(t_0), \dot{x}(t_0), \dot{y}(t_0), \dot{z}(t_0)]^T$. The eigenvalues of A are $\{\pm nj, \pm nj, 0, 0\}$, so a secular mode is expected to appear in the solution.

Solving the CW equations is straightforward. The solution may be formulated in terms of the transition matrix, $\mathrm{e}^{A(t-t_0)}$,

$$\mathbf{x}(t) = \mathrm{e}^{A(t-t_0)}\mathbf{x}(t_0) \tag{5.15}$$

Following the usual steps for computing the transition matrix yields (for $t_0 = 0$),

$$\mathrm{e}^{At} = \begin{bmatrix} 4 - 3\,\mathrm{c}_{nt} & 0 & 0 & \dfrac{\mathrm{s}_{nt}}{n} & \dfrac{2}{n} - \dfrac{2\mathrm{c}_{nt}}{n} & 0 \\ -6nt + 6\,\mathrm{s}_{nt} & 1 & 0 & -\dfrac{2}{n} + \dfrac{2\mathrm{c}_{nt}}{n} & \dfrac{4\mathrm{s}_{nt}}{n} - 3t & 0 \\ 0 & 0 & \mathrm{c}_{nt} & 0 & 0 & \dfrac{\mathrm{s}_{nt}}{n} \\ 3n\mathrm{s}_{nt} & 0 & 0 & \mathrm{c}_{nt} & 2\,\mathrm{s}_{nt} & 0 \\ -6n + 6n\mathrm{c}_{nt} & 0 & 0 & -2\,\mathrm{s}_{nt} & -3 + 4\,\mathrm{c}_{nt} & 0 \\ 0 & 0 & -n\mathrm{s}_{nt} & 0 & 0 & \mathrm{c}_{nt} \end{bmatrix} \tag{5.16}$$

We can now determine, by substituting Eq. (5.16) into Eq. (5.15), the solutions to the relative position and velocity components:

$$x(t) = \left[4x(0) + \frac{2\dot{y}(0)}{n}\right] + \frac{\dot{x}(0)}{n}\sin(nt) - \left[3x(0) + \frac{2\dot{y}(0)}{n}\right]\cos(nt) \quad (5.17)$$

$$y(t) = -[6nx(0) + 3\dot{y}(0)]t + \left[y(0) - \frac{2\dot{x}(0)}{n}\right] + \left[6x(0) + \frac{4\dot{y}(0)}{n}\right]\sin(nt) + \frac{2\dot{x}(0)}{n}\cos(nt), \quad (5.18)$$

$$z(t) = \frac{\dot{z}(0)}{n}\sin(nt) + z(0)\cos(nt), \quad (5.19)$$

$$\dot{x}(t) = \dot{x}(0)\cos(nt) + [3x(0)n + 2\dot{y}(0)]\sin(nt) \quad (5.20)$$

$$\dot{y}(t) = -[6nx(0) + 3\dot{y}(0)] + [6x(0)n + 4\dot{y}(0)]\cos(nt) - 2\dot{x}(0)\sin(nt) \quad (5.21)$$

$$\dot{z}(t) = \dot{z}(0)\cos(nt) - z(0)n\sin(nt) \quad (5.22)$$

A number of observations are in order. First, from the dynamical systems perspective, the linear system (5.13) has multiple equilibria $\{x = 0, y = \text{const.}, z = 0\}$, while the original, nonlinear system has a continuum of equilibria (4.77). There is some equivalence between the nonlinear and linear systems: In the linear system, the coordinate y can be written as $y = a\delta\theta$, where $\delta\theta$ is a curvilinear coordinate along the circumference of the reference orbit. Hence, $\delta\theta = \text{const.}$ corresponds to an angular shift of the deputy along the chief's reference orbit.

Second, we note that the linearization has decoupled the out-of-plane, *cross-track*, motion from the in-plane motion. The cross-track motion is a simple harmonic. It can be nullified by selecting the initial conditions: $z(0) = \dot{z}(0) = 0$.

Third, the transverse, *along-track*, component shows the presence of drift, varying linearly with time, implying that the in-plane motion is *unstable*. Nevertheless, we can find a *stable subspace* of the state-space, rendering the motion stable. The initial conditions which span the stable subspace are given by

$$\dot{y}(0) = -2nx(0) \quad (5.23)$$

Choosing initial conditions (5.23) will yield a bounded relative motion *to first order*, i.e., only for the CW model. It is important to note that the concept of stability in the context of the CW equations is *local*. There exist initial conditions which violate Eq. (5.23) but satisfy the energy matching condition, yielding a bounded 1:1 commensurable motion described by Eqs. (4.74)–(4.76). This is because the energy matching condition is a *global* boundedness criterion. By using the CW approximation, we truncate the physical solution of the problem, thus introducing an inherent error. The conclusions from the CW stability analysis must therefore be judiciously handled; it must be understood that the local results apply only in a small neighborhood of the chief, and cannot

be relied upon for drawing conclusions as to properties of the relative motion with respect to circular, two-body orbits.

Nevertheless, the stable CW solutions have some interesting geometric properties which are worth mentioning. To gain a geometric insight, note that if Eq. (5.23) is satisfied, Eqs. (5.17)–(5.19) may be written in the magnitude-phase form

$$x(t) = \rho_x \sin(nt + \alpha_x) \tag{5.24}$$

$$y(t) = \rho_y + 2\rho_x \cos(nt + \alpha_x) \tag{5.25}$$

$$z(t) = \rho_z \sin(nt + \alpha_z) \tag{5.26}$$

where

$$\rho_x = \frac{\sqrt{\dot{x}^2(0) + x^2(0)n^2}}{n} \tag{5.27}$$

$$\rho_y = [y(0) - 2\dot{x}(0)/n] \tag{5.28}$$

$$\rho_z = \frac{\sqrt{\dot{z}^2(0) + z^2(0)n^2}}{n} \tag{5.29}$$

$$\alpha_x = \tan^{-1} \frac{nx(0)}{\dot{x}(0)} \tag{5.30}$$

$$\alpha_z = \tan^{-1} \frac{nz(0)}{\dot{z}(0)} \tag{5.31}$$

Equations (5.24)–(5.26) constitute a parametric representation of an *elliptic cylinder*. If

$$\alpha_x = \alpha_z \tag{5.32}$$

then Eqs. (5.24)–(5.26) become a parametric representation of a 3D ellipse, generated by a section of the 3D cylinder, as shown in Fig. 5.1. This ellipse is centered on the y-axis at $(0, \rho_y, 0)$. If

$$\alpha_x = \alpha_z, \quad \rho_z = \sqrt{3}\rho_x \tag{5.33}$$

then the relative orbit is a 3D circle with radius $2\rho_x$. This relative orbit is commonly referred to as the *general circular orbit* (GCO).

In general, the xy-projection of the motion is a parametric representation of a 2:1 ellipse with semimajor axis $2\rho_x$, semiminor axis ρ_x and a constant eccentricity of $\sqrt{1 - \rho_x^2/(4\rho_x^2)} = \sqrt{3}/2$. The line of apsides is rotated $\pi/2$ radians relative to the y-axis, and the center of motion is located at the offset $[0, \rho_y]$.

The xz- and yz-projections are, in general, ovals. There are a few special cases, however, where these projections become elliptic, circular, or linear. An elliptic xz-projection is obtained if

$$\alpha_z = \pi/2 + \alpha_x \tag{5.34}$$

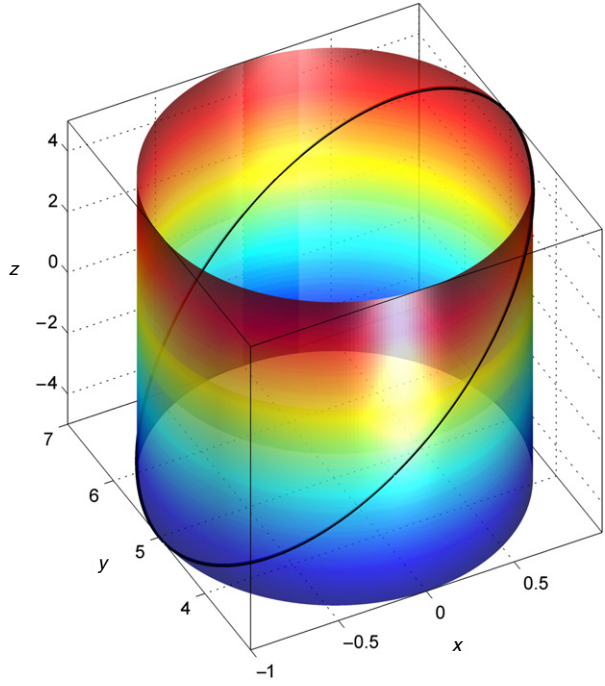

FIGURE 5.1 The bounded relative orbit in the linear approximation lies on a 3D elliptic cylinder. When the phases of the in-plane and out-of-plane motion match, the 3D relative orbit is a section of this cylinder.

and a circular xz-projection is obtained if

$$\alpha_z = \pi/2 + \alpha_x, \quad \rho_x = \rho_z \tag{5.35}$$

A linear xz projection is obtained if Eq. (5.32) holds. Equivalently, an elliptic yz-projection is obtained if Eq. (5.32) holds, and a circular yz-projection is obtained if

$$\alpha_x = \alpha_z, \quad \rho_z = 2\rho_x \tag{5.36}$$

The yz-circular-projection orbit, referred to as the *projected circular orbit* (PCO), has been the subject of a number of studies in the literature due to its potential applications, such as Earth-imaging. We will return to the PCO in Section 5.4. A linear yz-projection is obtained if Eq. (5.34) is satisfied.

For example, setting $x(0) = \dot{z}(0) = 0$ and $\dot{x}(0) = nz(0)$ yields a circular xz-projection and a linear yz-projection; setting $\dot{x}(0) = \dot{z}(0) = 0$ and $z(0) = 2x(0)$ yields a circular yz-projection and a linear xz projection.

Example 5.1. *Two satellites are launched aboard a Delta launcher. The satellites are to fly in a close formation. An initial velocity impulse injects the satellites into a circular LEO of* 600 km. *An additional velocity impulse applied by*

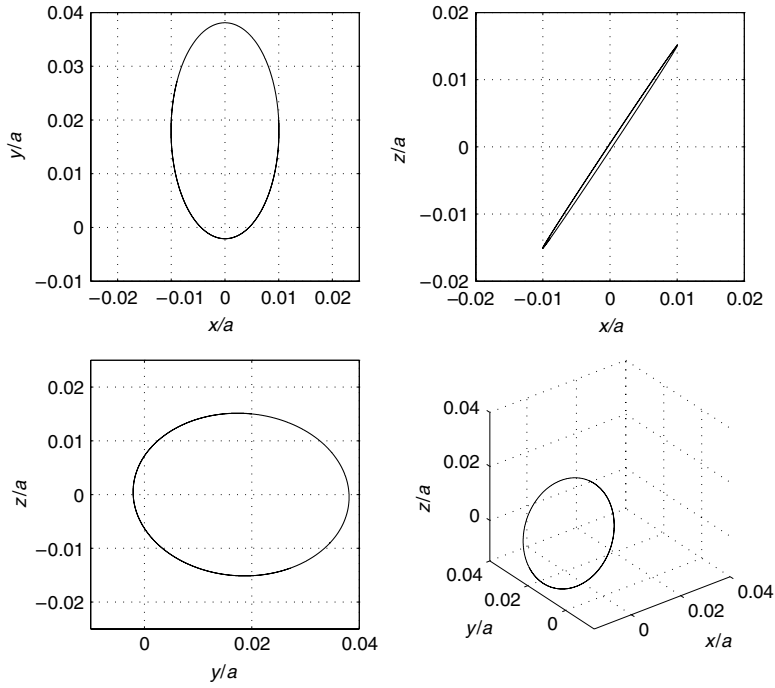

FIGURE 5.2 Geometry of a bounded relative orbit using the CW equations for relative motion. The xy-projection is a 2:1 ellipse.

the deputy de-attaches it from the chief so that the relative position components are

$$x(0) = 69.78 \text{ km}, \quad y(0) = 139.56 \text{ km}, \quad z(0) = 104.67 \text{ km}$$

and the relative velocity components are

$$\dot{x}(0) = 7.5579 \text{ m/s}, \quad \dot{y}(0) = -151.116 \text{ m/s}, \quad \dot{z}(0) = 15.116 \text{ m/s}$$

Determine the geometry of the relative orbit. What initial conditions should be chosen instead of the given initial conditions to yield circular xz- and yz-projections?

The satellite's orbit has $a = 600 + 6378 = 6978$ km, $n = \sqrt{3.986 \cdot 10^5/6978^3}$ rad/s. The relative position in normalized coordinates is thus $\bar{x}(0) = x(0)/a = 0.01$, $\bar{y}(0) = y(0)/a = 0.02$, $\bar{z}(0) = z(0)/a = 0.015$ and the normalized velocity is $\bar{x}'(0) = 0.001$, $\bar{y}'(0) = -0.002$, $\bar{z}'(0) = 0.002$. Simulating the CW equations with these initial conditions yields the geometry depicted in Fig. 5.2. The xy-projection of the relative orbit is clearly elliptic. In order to generate a circular xz-projection we need $\bar{x}(0) = 0$, $\bar{x}'(0) = \bar{z}(0) = 0.015$, $\bar{z}'(0) = 0$, and in order to generate a circular yz-projection (PCO), we should set $\bar{z}(0) = 2\bar{x}(0) = 0.02$, $\bar{x}'(0) = \bar{z}'(0) = 0$. The results are shown in Fig. 5.3 and Fig. 5.4, respectively. As expected, the circular xz-projection also

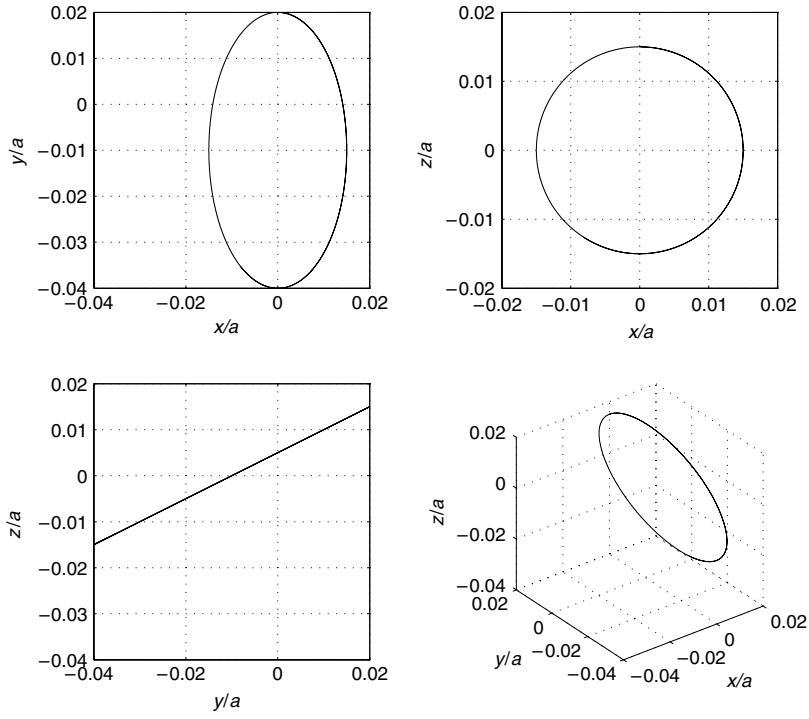

FIGURE 5.3 A circular xz-projection CW relative orbit.

yields a linear yz-projection. Similarly, the circular yz-projection yields a linear xz-projection. In both cases, of course, the projection on the xy plane is a 2:1 ellipse with eccentricity of $\sqrt{3}/2$.

5.2 TWO-IMPULSE LINEAR RENDEZVOUS

As we previously mentioned, the CW equations are linear, admitting an equilibrium at the origin (among other equilibria). Thus, a *ballistic* or *thrust-free* stable linear relative motion is possible if the chief and deputy spacecraft coincide. This is called *rendezvous*, that is, when both the relative position vector and relative velocity vector in the chief-fixed frame are nullified. Rendezvous has many practical applications and has been performed in numerous space missions. For example, docking of the Space Shuttle on the International Space Station requires a rendezvous maneuver.

It is therefore important to find impulsive velocity corrections that guarantee rendezvous. This will be performed in two stages: We will initially find an impulsive maneuver that nullifies the final relative distance between the chief and the deputy. This process is termed *targeting* or *guidance*. At the final time, once the relative distance has been nullified, we will determine the additional impulsive maneuver required to cancel the relative velocity and complete the rendezvous. This scheme is referred to as *two-impulse linear rendezvous*.

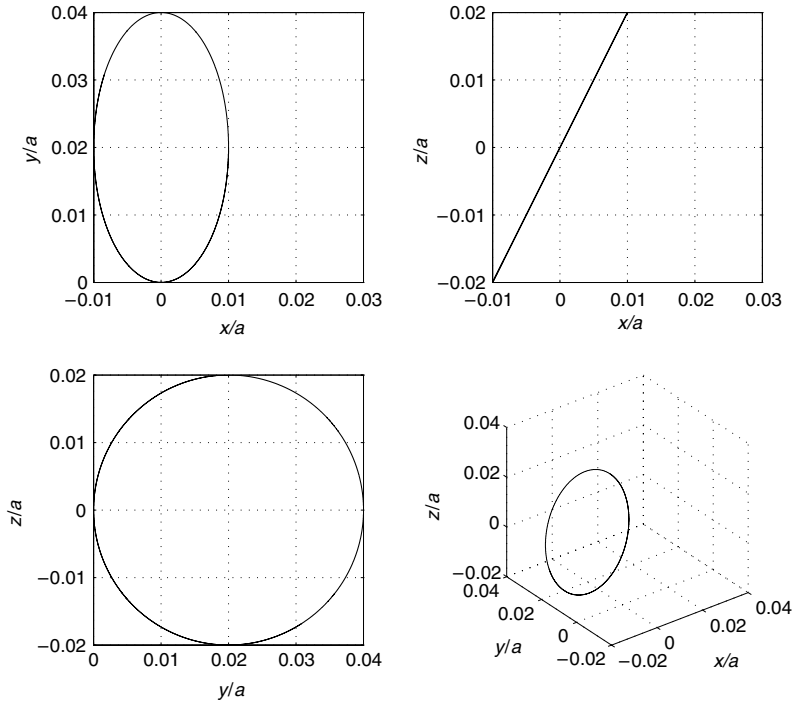

FIGURE 5.4 A circular zy-projection CW relative orbit (PCO).

Designating the moment of the targeting maneuver by $t_0 = 0$, the velocity impulse, $\Delta\mathbf{v}_I$, satisfies

$$\Delta\mathbf{v}_I = \mathbf{v}^+(0) - \mathbf{v}^-(0) \tag{5.37}$$

where $\mathbf{v}^-(0)$ and $\mathbf{v}^+(0)$ are the relative velocity vectors before and after application of the targeting impulse, respectively. The vector $\mathbf{v}^+(0)$, the required initial velocity for targeting, can be found by substituting $x(t_f) = y(t_f) = z(t_f) = 0$ into Eqs. (5.17)–(5.19) and solving for $\dot{x}(0)$, $\dot{y}(0)$, $\dot{z}(0)$, given the initial relative position components $x(0)$, $y(0)$, $z(0)$:

$$\begin{aligned}\mathbf{v}^+(0) &= \begin{bmatrix}\dot{x}(0)\\ \dot{y}(0)\\ \dot{z}(0)\end{bmatrix}^+ \\ &= \begin{bmatrix} -\dfrac{n\left[-4\,x(0)\,\mathrm{s}_{nt_f} + 3\,x(0)\,nt_f\,\mathrm{c}_{nt_f} + 2\,y(0) - 2\,y(0)\,\mathrm{c}_{nt_f}\right]}{-8 + 8\,\mathrm{c}_{nt_f} + 3\,nt_f\,\mathrm{s}_{nt_f}} \\ -\dfrac{n\left[-14\,x(0) + 14\,x(0)\,\mathrm{c}_{nt_f} + 6\,x(0)\,nt_f\,\mathrm{s}_{nt_f} - y(0)\,\mathrm{s}_{nt_f}\right]}{-8 + 8\,\mathrm{c}_{nt_f} + 3\,nt_f\,\mathrm{s}_{nt_f}} \\ -z(0)n\cot(nt_f)\end{bmatrix}\end{aligned} \tag{5.38}$$

$\mathbf{v}^+(0)$ does not exist for all flight times: $\dot{z}^+(0)$ is singular for $nt_f = k\pi, k = 0, 1, \ldots$, and the in-plane components $\dot{x}^+(0)$ and $\dot{y}^+(0)$ are singular at $nt_f = 2k\pi, k = 0, 1, \ldots$ and at additional points satisfying $8\mathrm{c}_{nt_f} + 3nt_f\mathrm{s}_{nt_f} = 8$ such as $nt_f = 2.8135\pi$ and $nt_f = 4.8906\pi$.

At t_f, when the deputy satellite – a *chaser* or a *pursuer* – reaches the chief satellite – a *target*, its relative velocity must be nullified to guarantee rendezvous. Therefore, the required velocity impulse at impact must be equal in magnitude and opposite in sign to the final relative velocity:

$$\Delta\mathbf{v}_{II} = -\mathbf{v}(t_f) \tag{5.39}$$

where $\mathbf{v}(t_f)$ is the final relative velocity, obtained by substituting $t = t_f$ into Eqs. (5.20)–(5.22),

$$\begin{aligned}\mathbf{v}(t_f) &= \begin{bmatrix}\dot{x}(t_f)\\ \dot{y}(t_f)\\ \dot{z}(t_f)\end{bmatrix}\\ &= \begin{bmatrix}\dot{x}^+(0)\mathrm{c}_{nt_f} + [3x(0)n + 2\dot{y}^+(0)]\mathrm{s}_{nt_f}\\ -[6nx(0) + 3\dot{y}^+(0)] + [6x(0)n + 4\dot{y}^+(0)]\mathrm{c}_{nt_f} - 2\dot{x}^+(0)\mathrm{s}_{nt_f}\\ \dot{z}^+(0)\mathrm{c}_{nt_f} - z(0)n\mathrm{s}_{nt_f}\end{bmatrix}\end{aligned} \tag{5.40}$$

The total velocity change required for a two-impulse rendezvous is

$$\Delta v = \|\Delta\mathbf{v}_I\| + \|\Delta\mathbf{v}_{II}\| \tag{5.41}$$

In Eq. (5.41), the vector norm depends on the type of thrusters used. If the thrust is applied using a single directional thruster, one must take $\|\cdot\|_2$; if a cluster of body-fixed thrusters are used, providing the required thrust components in each direction, one must substitute $\|\cdot\|_1$ into Eq. (5.41). A good discussion of this topic can be found in Ref. [103].

Example 5.2. *A satellite is in a circular LEO of* 600 km. *The Space Shuttle is launched to retrieve the satellite. At* $t = 0$*, a laser ranging system on board the shuttle determines that the relative separation between the Shuttle bay and the satellite is*

$$x(0) = 69.78 \text{ km}, \quad y(0) = 139.56 \text{ km}, \quad z(0) = 104.67 \text{ km}$$

and that the relative velocity is

$$\dot{x}(0) = \dot{y}(0) = \dot{z}(0) = 7.5579 \text{ m/s}$$

Determine the components and the magnitude of the impulsive velocity corrections required for rendezvous after 3.22 hours.

Let us first normalize the given quantities. The satellite's orbit radius is $a = 600+6378 = 6978$ km, and the mean motion is $n = \sqrt{3.986 \cdot 10^5/6978^3}$ rad/s.

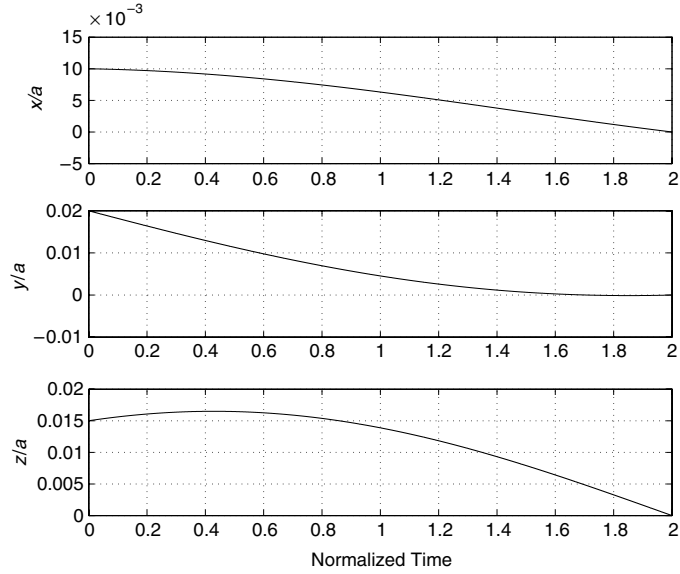

FIGURE 5.5 The relative position components converge to zero following an application of an impulsive targeting maneuver.

The relative position in normalized coordinates is therefore $x(0)/a = 0.01$, $y(0)/a = 0.02$, $z(0)/a = 0.015$ and the normalized velocity is $\bar{x}'(0) = \bar{y}'(0) = \bar{z}'(0) = 7.5579/(na) = 0.001$. The normalized retrieval time is $3.22 \cdot 3600 \cdot n/(2\pi) = 2$. Substituting the data into Eq. (5.38) gives the normalized velocity corrections

$$\Delta\bar{\mathbf{v}}_I = \begin{bmatrix} -0.00178 \\ -0.01927 \\ 0.005865 \end{bmatrix}, \tag{5.42}$$

The normalized final velocity change is computed according to Eq. (5.40),

$$\Delta\bar{\mathbf{v}}_{II} = \begin{bmatrix} -0.00562 \\ 0.00173 \\ -0.0165 \end{bmatrix}, \tag{5.43}$$

Assuming a directional thruster, the total normalized velocity change required is $\Delta\bar{v} = \|\Delta\bar{\mathbf{v}}_I\|_2 + \|\Delta\bar{\mathbf{v}}_{II}\|_2 = 0.03774$. A simulation of the rendezvous has been carried out in MATLAB®. Figure 5.5 depicts the relative position components, showing convergence to zero relative position at the normalized time $\bar{t} = 2$, as expected. Figure 5.6 shows the relative velocity components and the impulsive velocity correction at impact, which nullifies the final values of the relative velocity to yield perfect rendezvous.

From the above discussion, it is obvious that the total velocity change required for rendezvous strongly depends on the time of flight. We can thus ask

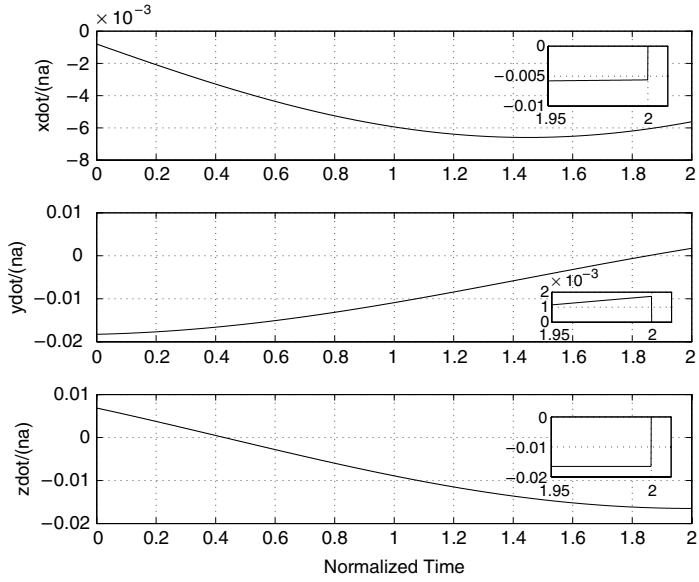

FIGURE 5.6 The relative velocity components are nullified at impact to guarantee rendezvous. A magnified view shows the impulsive velocity correction.

whether there exists a t_f for which the required Δv is minimal given the initial conditions (5.2). We may attempt to answer this query analytically, perform a batch of simulations or simulate the adjoint system to discover the optimum flight time. Adopting the latter approach, we plotted the total Δv vs. t_f and obtained the desired optimum t_f (in normalized units). Figure 5.7 shows a plot of $\Delta\bar{v}$ vs. $\bar{t}_f$. $\Delta\bar{v}$ is maximal near the singularities mentioned above. The minimal velocity change, $\Delta\bar{v} = 0.0375$, is achieved at $\bar{t}_f \approx 4.65$.

We should highlight the fact that the rendezvous methodology implemented in this section relies on the CW equations, and is hence limited to circular unperturbed target orbits. More general solution s for the rendezvous problems have been obtained, see e.g., Ref. [104] (and references therein), in which a bounded solution for the rendezvous problem was derived by neglecting second-order eccentricity terms in the approximation of the chaser's orbit.

To conclude this section, we point out that implementing a certain Δv plan relies upon measuring the specific thrust using, e.g., accelerometers. The challenges associated with this issue are discussed in Chapter 11.

5.3 LAGRANGIAN AND HAMILTONIAN DERIVATIONS OF THE CW EQUATIONS

As in the treatment of Section 5.1, leading to the CW equations, we examine only small deviations from the reference orbit. Thus, we only consider the first three terms of the potential energy (4.84) (here, again, we use the notation

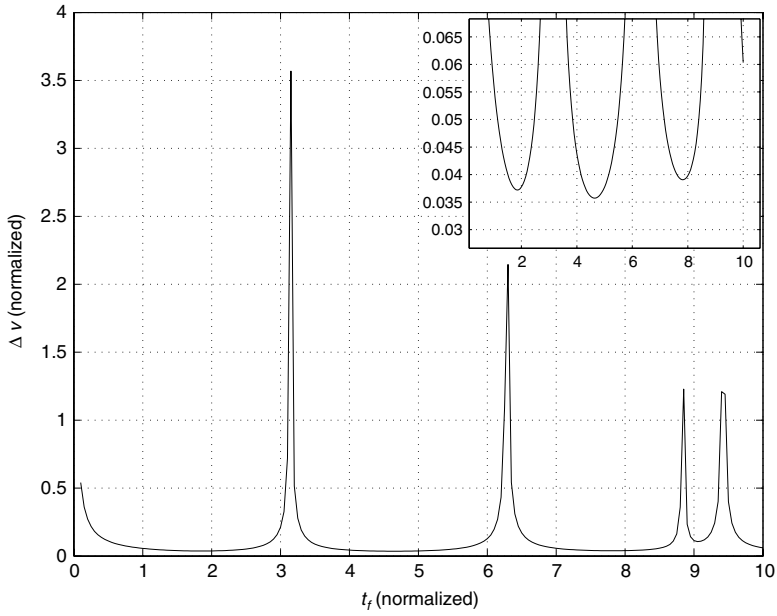

FIGURE 5.7 The total velocity change required for rendezvous varies with the time of flight. The global minimum for the initial conditions given in Example 5.2 is at $t_f \approx 4.65$, as shown in the top right pane.

$n \equiv n_0$ and $a \equiv a_0$)

$$\mathcal{U}^{(0)} = -\frac{\mu}{a} - \frac{\mu}{a^2}\rho\cos\vartheta - \frac{\mu}{a^3}\rho^2\left(\frac{3}{2}\cos^2\vartheta - \frac{1}{2}\right) \tag{5.44}$$

and then use Eq. (4.85) to find the low order Lagrangian,

$$\begin{aligned}\mathcal{L}^{(0)} = {} & \frac{1}{2}\left(\dot{x}^2 + \dot{y}^2 + \dot{z}^2\right) + n\left(x\dot{y} - y\dot{x} + a\dot{y}\right) \\ & + \frac{3}{2}n^2a^2 + \frac{3}{2}n^2x^2 - \frac{n^2}{2}z^2\end{aligned} \tag{5.45}$$

with the perturbed part of the Lagrangian equal to the higher-order terms in the potential $[\mathcal{O}((\rho/a)^3)]$. Omitting the details, it is straightforward to derive the usual CW equations using the Euler–Lagrange equations (3.3):

$$\ddot{x} - 2n\dot{y} - 3n^2x = 0 \tag{5.46}$$

$$\ddot{y} + 2n\dot{x} = 0 \tag{5.47}$$

$$\ddot{z} + n^2z = 0 \tag{5.48}$$

It is helpful before proceeding further to normalize our equations and simplify the notation. Normalizing rates by n (so time is in fractions of an orbit) and

relative distances by a, the normalized Lagrangian is given by:

$$\bar{\mathcal{L}}^{(0)} = \frac{1}{2}\left[(\bar{x}')^2 + (\bar{y}')^2 + (\bar{z}')^2\right] + \left[(\bar{x}+1)\bar{y}' - \bar{y}\bar{x}'\right] + \frac{3}{2} + \frac{3}{2}\bar{x}^2 - \frac{1}{2}\bar{z}^2 \tag{5.49}$$

We can also obtain the equivalent three-degrees-of-freedom normalized Hamiltonian $\bar{\mathcal{H}}^{(0)} : \mathbb{R}^3 \times \mathbb{R}^3 \to \mathbb{R}$ for the linear relative motion dynamics. The canonical momenta are found from the usual definition:

$$\begin{aligned} p_x &= \frac{\partial \bar{\mathcal{L}}^{(0)}}{\partial \bar{x}'} = \bar{x}' - \bar{y} \\ p_y &= \frac{\partial \bar{\mathcal{L}}^{(0)}}{\partial \bar{y}'} = \bar{y}' + \bar{x} + 1 \\ p_z &= \frac{\partial \bar{\mathcal{L}}^{(0)}}{\partial \bar{z}'} = \bar{z}' \end{aligned} \tag{5.50}$$

and then, using the Legendre transformation, the normalized Hamiltonian for linear relative motion in Cartesian coordinates is obtained as

$$\bar{\mathcal{H}}^{(0)} = \frac{1}{2}(p_x + \bar{y})^2 + \frac{1}{2}(p_y - \bar{x} - 1)^2 + \frac{1}{2}p_z^2 - \frac{3}{2} - \frac{3}{2}\bar{x}^2 + \frac{1}{2}\bar{z}^2 \tag{5.51}$$

The *linear Hamiltonian equations of relative motion* (in normalized form) are derived from $\bar{\mathcal{H}}^{(0)}$ using Hamilton's equations (3.6):

$$\bar{x}' = p_x + \bar{y} \tag{5.52}$$
$$\bar{y}' = p_y - \bar{x} - 1 \tag{5.53}$$
$$\bar{z}' = p_z \tag{5.54}$$
$$p_x' = p_y + 2\bar{x} - 1 \tag{5.55}$$
$$p_y' = -p_x - \bar{y} \tag{5.56}$$
$$p_z' = -\bar{z} \tag{5.57}$$

It is informative to rewrite $\bar{\mathcal{H}}^{(0)}$ in the tangent space as shown below:

$$\bar{\mathcal{H}}^{(0)} = \frac{1}{2}\left[(\bar{x}')^2 + (\bar{y}')^2 + (\bar{z}')^2\right] - \frac{3}{2} - \frac{3}{2}\bar{x}^2 + \frac{1}{2}\bar{z}^2 \tag{5.58}$$

For the special case of periodic orbits, satisfying Eq. (5.23), the above equation becomes

$$\bar{\mathcal{H}}^{(0)} = \frac{1}{2}\left[(\bar{x}')^2 + (\bar{z}')^2\right] + \frac{1}{2}(\bar{x}^2 + \bar{z}^2) - \frac{3}{2} \tag{5.59}$$

Ignoring the constant term $(-3/2)$ in Eq. (5.59), we note that the special case $\bar{\mathcal{H}}^{(0)}$ provides a positive definite function in the reduced configuration space

(y is a dependent function of x); such a function can serve as a Lyapunov function for the CW equations, as long as Eq. (5.23) is satisfied. In general, the Hamiltonian cannot serve as a Lyapunov function for an autonomous dynamical system.

The Lagrangian and Hamiltonian formalisms can be used to obtain corrections for the initial conditions guaranteeing bounded motion in the CW relative motion model. This is performed by taking third-order expressions in the Legendre polynomial expansion of the differential gravitational potential, as shown in the next section.

5.4 ACCOMMODATING SECOND-ORDER NONLINEARITIES

Equations (4.74)–(4.76) can be approximated by either a second-order expansion of the differential gravitational acceleration about a circular orbit, or by taking third-order expressions in the Legendre-polynomial expansion of the Lagrangian, as discussed in Chapter 4. This procedure leads to the following equations, written using normalized coordinates and non-dimensional time:

$$\begin{aligned} \bar{x}'' - 2\bar{y}' - 3\bar{x} &= \left[\frac{\bar{y}^2}{2} + \frac{\bar{z}^2}{2} - \bar{x}^2\right] \\ \bar{y}'' + 2\bar{x}' &= 3\bar{x}\bar{y} \\ \bar{z}'' &= 3\bar{x}\bar{z} \end{aligned} \tag{5.60}$$

It is useful to compare these equations to the normalized CW equations (5.10)–(5.12). Equation (5.60) can be obtained from the normalized Lagrangian [105]

$$\begin{aligned} \bar{\mathcal{L}}^{(1)} = \frac{1}{2}\left[(\bar{x}')^2 + (\bar{y}')^2 + (\bar{z}')^2\right] + \left[\bar{x}\bar{y}' - \bar{y}\bar{x}'\right] + \frac{1}{2}(3\bar{x}^2 - \bar{z}^2) \\ - \frac{1}{2}(2\bar{x}^3 - 3\bar{x}\bar{y}^2 - 3\bar{x}\bar{z}^2) \end{aligned} \tag{5.61}$$

A perturbation method for accommodating the effects of second-order nonlinearities in the design of periodic relative orbits was put forth by Vaddi et al. [106]. They obtained a first-order perturbation solution to Eq. (5.60) and showed that the initial conditions provided by the CW solutions can be corrected to achieve bounded relative orbits. Their correction equation, in dimensional form, is

$$\begin{aligned} &\dot{y}(0) + 2nx(0) \\ &\quad + \frac{3n}{2a}\left(2{\rho_x}^2 + 2{\rho_y}^2 + {\rho_z}^2 + 6\rho_x\rho_y\cos\alpha_x + 3{\rho_x}^2\cos 2\alpha_x\right) = 0 \end{aligned} \tag{5.62}$$

where ρ_x, ρ_y, and ρ_z are the constants describing the CW solutions, as discussed in Section 5.1 (Eqs. (5.24)–(5.26)). Note that α_z does not affect the above

solution. Equation (5.62) can be satisfied by selecting either $x(0)$ or $\dot{y}(0)$. Furthermore, Eq. (5.62) can also be utilized to estimate the effect of nonlinearity on secular along-track growth. If Eq. (5.23) is satisfied, an estimate of the along-track drift rate due to nonlinearity, obtained from Eq. (5.62), is

$$\dot{y}_{\text{drift}} = -\frac{3n}{2a}(2{\rho_x}^2 + 2{\rho_y}^2 + {\rho_z}^2 + 6\rho_x\rho_y\cos\alpha_x + 3{\rho_x}^2\cos 2\alpha_x) \quad (5.63)$$

Specializing Eq. (5.63) to the case of a PCO with $2\rho_x = \rho_z \equiv \rho$, $\rho_y = 0$, and $\alpha_x = \alpha_z \equiv \alpha$, a linear estimate of the along-track drift per orbit is

$$y_{\text{drift}} = -\frac{9\pi\rho^2}{4a_0}(2 + \cos 2\alpha) \quad (5.64)$$

Example 5.3. *For a circular orbit with* $a_0 = 7100$ km, $\rho = 1$ km, *the drift rate is approximately equal to* 3 m *per orbit, for* $\alpha = 0°$ *and* 1 m *per orbit, for* $\alpha = 90°$.

A perturbation solution based on Eq. (5.60) for the differential energy between two satellites in a formation can be derived from the more general results of Ref. [107] as follows:

$$\delta\bar{\mathcal{E}} = (\bar{y}' + 2\bar{x}) + \frac{1}{2}\left[(\bar{x}' - \bar{y})^2 + (\bar{y}' + \bar{x})^2 + (\bar{z}')^2 - \left(2\bar{x}^2 - \bar{y}^2 - \bar{z}^2\right)\right] \quad (5.65)$$

An alternate approach, followed by Jiang et al. [108], is to approximate the differential semimajor axis, δa, by a Taylor series expansion of a_1 (calculated from Eq. (4.34)) about the semimajor axis of the chief. For example, a linear approximation valid for circular reference orbits, written in non-dimensional coordinates, is

$$\delta\bar{a}^{(1)} = 2(\bar{y}' + 2\bar{x}) \quad (5.66)$$

A second-order expansion for δa is

$$\delta\bar{a}^{(2)} = \delta\bar{a}^{(1)} + \left[\left(\delta\bar{a}^{(1)}\right)^2 + (\bar{x}' - \bar{y})^2 + (\bar{y}' + \bar{x})^2 + \bar{z}^2 - \left(2\bar{x}^2 - \bar{y}^2 - \bar{z}^2\right)\right] \quad (5.67)$$

It can be shown by expanding the normalized form of the energy equation (2.25) that the expressions (5.65) and (5.67) are related as

$$\delta\bar{a}^{(2)} \approx 2\left[\delta\bar{\mathcal{E}} + 2\left(\delta\bar{\mathcal{E}}\right)^2\right] \quad (5.68)$$

For circular reference orbits, a linear estimate of the non-dimensional along-track drift rate due to second-order nonlinear effects can be obtained from the

non-dimensional δa via the relationship

$$\bar{y}' = -\frac{3}{2}\delta\bar{a} \tag{5.69}$$

The presentation in this section shows that expressions for the along-track drift rates due to linearization, or corrections for accommodating the nonlinear effects can be arrived at in several ways. For example, Eq. (5.63) can be obtained from Eqs. (5.69) and (5.67). More general treatments of the $\delta\mathcal{E}$ and δa expressions for eccentric orbits, involving f and e of the chief as parameters, can be found in Refs. [107,108].

5.5 CURVILINEAR VS. CARTESIAN RELATIVE COORDINATES

As we have seen in Section 5.1, the CW equations express the relative motion with respect to a rotating Cartesian coordinate system whose origin coincides with the chief satellite. The assumptions made in their derivation are that (a) the reference of chief orbit is circular, (b) the Earth is spherically symmetric, and (c) the distance between the chief and deputy is small compared to the radius of the orbit so that only the linear terms in the expansion of the differential gravity are retained. In this section, we explore some effects of the linearization assumption and show how to minimize the effect of the neglected nonlinear terms using a change in variables.

In the derivation of the CW equations, a linearization is performed in the expansion of the differential gravity, as shown earlier in Section 5.1. However, the initial conditions are also affected; this happens when obtaining the relative initial conditions from the exact inertial initial conditions of both satellites, or when obtaining the exact initial conditions of the deputy from the chief's initial conditions and the deputy's relative initial conditions.

To illustrate this initial condition impact, consider a simple example of co-orbital motion. The chief is in a circular orbit of radius a_0 and the deputy is in the same orbit, but leading the chief by an angle ς, as shown in Fig. 5.8. Now, obtain the exact relative initial conditions for the deputy. To that end, we first establish an inertial coordinate system, (X, Y, Z), whose axes are aligned at this instant with the LVLH system (x, y, z), but its origin is at the center of the Earth. The initial conditions of the deputy in the $\mathscr{I}$ frame are

$$\begin{aligned} X(0) &= a_0 \cos\varsigma, \quad \dot{X}(0) = -a_o n \sin\varsigma \\ Y(0) &= a_0 \sin\varsigma, \quad \dot{Y}(0) = a_0 n \cos\varsigma \\ Z(0) &= 0, \quad \dot{Z}(0) = 0 \end{aligned} \tag{5.70}$$

The corresponding initial conditions in the relative frame are

$$\begin{aligned} x(0) &= a_0\,(\cos\varsigma - 1)\,, \quad \dot{x}(0) = 0 \\ y(0) &= a_0 \sin\varsigma, \quad \dot{y}(0) = 0 \\ z(0) &= 0, \quad \dot{z}(0) = 0 \end{aligned} \tag{5.71}$$

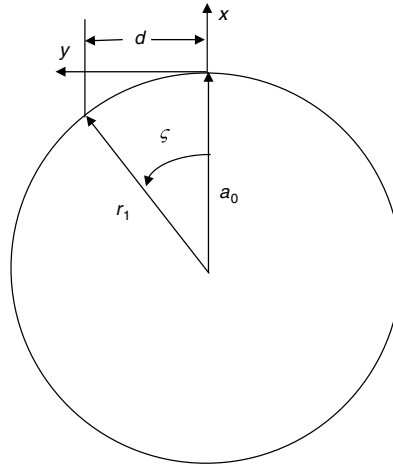

FIGURE 5.8 A simple example of leader–follower co-orbital formation.

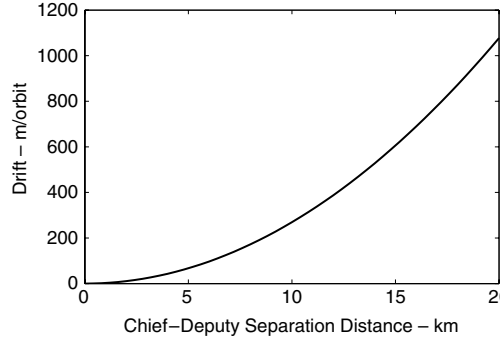

FIGURE 5.9 Drift per orbit caused by the CW equations initial conditions.

The differential semimajor axis resulting from these initial conditions is

$$\delta a = 4x(0) + 2\dot{y}(0)/n_0 = 4a_0(\cos\varsigma - 1) \approx -2a_0\varsigma^2 \tag{5.72}$$

Thus, the secular term coefficient in Eq. (5.18) is not zero. The secular in-track drift per orbit is

$$3\pi\delta a = 12\pi a_0(1 - \cos\varsigma) \approx 6\pi a_0\varsigma^2 \tag{5.73}$$

Example 5.4. *Evaluate the drift per orbit caused by the CW initial conditions for an initial along-track separation and a circular chief orbit of* $a_0 = 7000$ km *based on Eq.* (5.73).

Figure 5.9 shows the along-track drift per orbit that occurs when using the relative Cartesian reference frame for selecting the initial conditions. A drift of 269 m/orbit occurs for a 10 km initial separation. This drift would have to be negated by control.

The inverse scenario, that of starting with the initial relative state and obtaining the initial state of the deputy in the $\mathscr{I}$ frame, has a similar problem. With the same problem of a leader–follower formation with an along-track separation $D \approx a_0\varsigma$, as shown in Fig. 5.8, the radius of the deputy's orbit is

$$r_1 = \left(a_0^2 + D^2\right)^{1/2} \approx a_0\left[1 + 0.5\,(D/a_0)^2\right] \tag{5.74}$$

Thus

$$\delta r \approx 0.5 a_0 \varsigma^2 \tag{5.75}$$

The deputy velocity is

$$v = \left[(a_0 n_0)^2 + (D n_0)^2\right] \tag{5.76}$$

From the vis-viva equation (2.14),

$$-\frac{\mu}{a} = v^2 - 2\frac{\mu}{r}$$

we can write

$$\frac{\mu}{a_0^2}\delta a = 2v\delta v + 2\frac{\mu}{r_0^2}\delta r \tag{5.77}$$

and hence

$$\delta a = 2a_0 \sin\varsigma^2 \approx 2a_0\varsigma^2 \tag{5.78}$$

Comparing to Eq. (5.72), we see that δa has the same magnitude, but opposite sign. Therefore, the same drift occurs whether or not the deputy's relative initial conditions are obtained from the exact initial conditions of the chief and deputy, or the deputy's exact initial conditions are obtained from the chief's exact and deputy's relative initial conditions. If the initial radius and the corresponding initial relative states are used as the initial conditions for numerical integration or an analytic theory, the two satellites will slowly drift apart, even though they are in the same orbit. Thus, the use of the Cartesian rotating coordinate system results in undesirable errors in the solution due to the nonlinear terms. These nonlinear effects can be reduced if a curvilinear coordinate system is used, as we show now.

To that end, let $(\delta r, \theta_r, \phi_r)$ be the relative coordinates, as shown in Fig. 5.10, where δr is the difference between the radii of the deputy and chief, θ_r is the angle between the projection of the deputy's radius vector in the chief's orbit plane and the chief's radius vector, and ϕ_r is the angle between deputy's radius vector and its projection in the chief's orbit plane. Thus, $(\delta r, a_0\theta_r, a_0\phi_r)$ are analogous to (x, y, z). The radius and velocity vectors of the deputy are

$$\mathbf{r}_1 = r_1\hat{\mathbf{r}}_1 = (a_0 + \delta r)\,\hat{\mathbf{r}}_1 \tag{5.79}$$

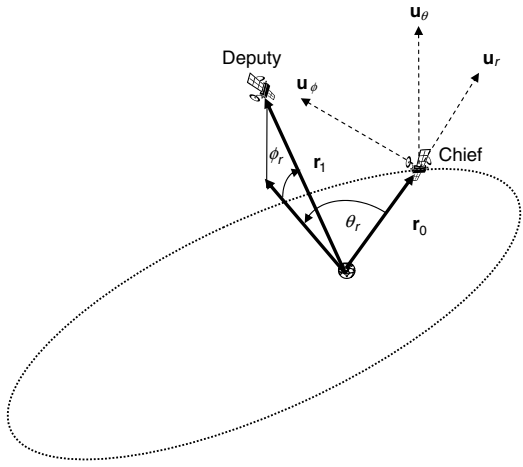

FIGURE 5.10 Relative curvilinear coordinate system.

$$\mathbf{v}_1 = \delta\dot{r}\hat{\mathbf{r}}_1 + (a_0 + \delta r)\,\boldsymbol{\omega}_1 \times \hat{\mathbf{r}}_1 \tag{5.80}$$

where

$$\begin{aligned} \boldsymbol{\omega}_1 &= \boldsymbol{\omega}_0 + \boldsymbol{\omega}_{1/0} \\ \boldsymbol{\omega}_0 &= n_0\hat{\mathbf{u}}_\phi \\ \boldsymbol{\omega}_{1/0} &= \dot{\theta}_r\hat{\mathbf{u}}_\phi + \dot{\phi}_r\left(\hat{\mathbf{u}}_\theta\cos\theta_r - \hat{\mathbf{u}}_r\sin\theta_r\right) \end{aligned} \tag{5.81}$$

$$\hat{\mathbf{r}}_1 = \hat{\mathbf{u}}_r\cos\phi_r\cos\theta_r - \hat{\mathbf{u}}_\theta\cos\phi_r\sin\theta_r - \hat{\mathbf{u}}_\phi\sin\phi_r \tag{5.82}$$

The acceleration of the deputy is

$$\ddot{\mathbf{r}}_1 = \delta\ddot{r}\hat{\mathbf{r}}_1 + 2\delta\dot{r}\boldsymbol{\omega}_1 \times \hat{\mathbf{r}}_1 + r_1\dot{\boldsymbol{\omega}}_1 \times \hat{\mathbf{r}}_1 + r_1\boldsymbol{\omega}_1 \times \left(\boldsymbol{\omega}_1 \times \hat{\mathbf{r}}_1\right) \tag{5.83}$$

where

$$\begin{aligned} \dot{\boldsymbol{\omega}}_1 = {} & \ddot{\theta}_r\hat{\mathbf{u}}_r + \ddot{\phi}_r\left(\hat{\mathbf{u}}_\theta\cos\theta_r - \hat{\mathbf{u}}_r\sin\theta_r\right) \\ & - \dot{\theta}_r\dot{\phi}_r\left(\hat{\mathbf{u}}_r\cos\theta_r + \hat{\mathbf{u}}_\theta\sin\theta_r\right) + \boldsymbol{\omega}_0 \times \boldsymbol{\omega}_{1/0} \end{aligned} \tag{5.84}$$

Note that in the curvilinear coordinate formulation there are nonlinear terms in the kinematic equation, whereas in the Cartesian formulation the kinematic equation is linear. Substituting Eqs. (5.81) and (5.84) into Eq. (5.83) and linearizing in δr, θ_r and ϕ_r gives

$$\begin{aligned} \ddot{\mathbf{r}}_1 = {} & \left(\delta\ddot{r}_1 - 2n_0a_0\dot{\theta}_r - n_0^2\delta r - n_0^2a_0\right)\hat{\mathbf{u}}_r \\ & + \left(a_0\ddot{\theta}_r + 2a_0n_0\delta\dot{r} - a_0n_0^2\theta_r\right)\hat{\mathbf{u}}_\theta - a_0\ddot{\phi}_r\hat{\mathbf{u}}_\phi \end{aligned} \tag{5.85}$$

The gravitational acceleration is

$$-\frac{\mu}{r_1^2}\hat{\mathbf{r}}_1 = -\frac{\mu}{(a_0+\delta r)^2}\hat{\mathbf{r}}_1 \tag{5.86}$$

Expanding the denominator in a Taylor series in δr, substituting for $\hat{\mathbf{r}}_1$ and linearizing in δr, θ_r and ϕ_r gives

$$-\frac{\mu}{r_1^2}\hat{\mathbf{r}}_1 = -n_0^2\left(a_0\hat{\mathbf{u}}_r - 2\delta r\hat{\mathbf{u}}_r - a_0\theta_r\hat{\mathbf{u}}_\theta - a_0\phi_r\hat{\mathbf{u}}_\phi\right) \tag{5.87}$$

Equating Eqs. (5.85) and (5.87) gives the equations of relative motion in curvilinear coordinates:

$$\begin{aligned}
&\delta\ddot{r} - 2a_0n_0\dot{\theta}_r - 3n_0^2\delta r = 0\\
&a_0\ddot{\theta}_r - 2n_0\delta\dot{r} = 0\\
&\ddot{\phi}_r + n_0^2\phi_r = 0
\end{aligned} \tag{5.88}$$

Note that these equations are identical to the CW equations with (x, y, z) being replaced by $(\delta r, a_0\theta_r, a_0\phi_r)$. The difference is that the along-track and cross-track distances are measured along arc lengths; they are not linear displacements. This reduces the nonlinear effects in the computation of the initial conditions. Another way to look at this (when using the CW equations) is to let x be the radii difference, y be the arc length displacement along the chief orbit, and z be the arc length displacement in the cross-track direction. Due to the linearization there will still be errors that occur with the use of the curvilinear coordinate equations, but the errors are much smaller. In addition to the effect of the neglected nonlinearities in the initial conditions, there are the neglected nonlinearities that occur from the expansion of the differential gravity. The use of the curvilinear coordinates also reduces these effects.

5.6 ELLIPTIC REFERENCE ORBITS

For circular reference orbits, the choice of the independent variable of either time or true anomaly leads to the same form of the equations of motion. This is not the case for elliptic reference orbits. Time-explicit solutions are attractive since Kepler's equation need not be solved to produce results at specified points of time. However, true-anomaly-based solutions have certain advantages, especially near the perigee, and are more suitable for long-term motion prediction for elliptic orbits.

5.6.1 Time as the independent variable: Melton's STM

Melton [109] has developed expansions of the STM in powers of eccentricity, in both Cartesian as well as cylindrical coordinate systems. A brief outline of his approach is presented here. The linearized equations of relative motion with respect to an unperturbed eccentric reference orbit in a Cartesian coordinate

system can be obtained from Eqs. (4.14)–(4.16) as follows (note that the linearization is with respect to the orbit of the chief):

$$\ddot{x} - 2\dot{\theta}\dot{y} - \ddot{\theta}y - \dot{\theta}^2 x = \frac{2\mu x}{r^3} \tag{5.89a}$$

$$\ddot{y} + 2\dot{\theta}\dot{x} + \ddot{\theta}x - \dot{\theta}^2 y = -\frac{\mu y}{r^3} \tag{5.89b}$$

$$\ddot{z} = -\frac{\mu z}{r^3} \tag{5.89c}$$

For unperturbed motion, using the result

$$r^2 = \frac{h}{\dot{\theta}} \tag{5.90}$$

where h is the angular momentum, Eqs. (5.89) can also be written as

$$\ddot{x} = \left[\dot{\theta}^2 + \frac{2\mu}{h^{3/2}}\dot{\theta}^{3/2}\right] x + \ddot{\theta}y + 2\dot{\theta}\dot{y} \tag{5.91a}$$

$$\ddot{y} = -\ddot{\theta}x + \left[\dot{\theta}^2 - \frac{\mu}{h^{3/2}}\dot{\theta}^{3/2}\right] y - 2\dot{\theta}\dot{x} \tag{5.91b}$$

$$\ddot{z} = -\left[\frac{\mu}{h^{3/2}}\dot{\theta}^{3/2}\right] z \tag{5.91c}$$

The equations of motion in the cylindrical coordinate system are obtained from Eq. (5.91) by using non-dimensional in-plane variables $\bar{x} = x/r$ and $\bar{y} = y/r$. Regardless of the coordinate system utilized, the linearized equations can be written in matrix form as follows:

$$\dot{\mathbf{x}}(t) = A(t)\mathbf{x}(t) \tag{5.92}$$

where the state vector is defined as

$$\mathbf{x} = [x, y, z, \dot{x}, \dot{y}, \dot{z}]^T \tag{5.93}$$

The variables r and $\dot{\theta}$ can be expanded in powers of eccentricity, as shown in Battin [33]:

$$r = a[1 - e\cos M - 1/2e^2(\cos 2M - 1) + \cdots] + \mathcal{O}(e^3) \tag{5.94a}$$

$$\dot{\theta} = n[1 + 2e\cos M + 5/2e^2\cos 2M] + \mathcal{O}(e^3) \tag{5.94b}$$

Since $A(t)$ consists of periodic terms, it can also be expanded in powers of e:

$$A(t) = A_0 + eA_1(t) + e^2A_2(t) + \cdots \tag{5.95}$$

where A_0 is a constant matrix and $A_{1,2,\ldots}$ are functions of time. In a similar fashion, the STM can also be expanded as shown below:

$$\Phi(t, t_0) = \Phi_0(t, t_0) + e\Phi_1(t, t_0) + e^2\Phi_2(t, t_0) + \cdots \tag{5.96}$$

where

$$\Phi_0(t, t_0) = \exp[A_0(t - t_0)] \tag{5.97}$$

Since the STM of Eq. (5.92) also satisfies the same differential equation, direct substitution of Eqs. (5.95) and (5.96) yields

$$\begin{aligned}\dot{\Phi}(t, t_0) &= A\Phi(t, t_0) \\ &= [A_0 + eA_1(t) + \cdots] \times [\Phi_0(t, t_0) + e\Phi_1(t, t_0) + \cdots] \end{aligned} \tag{5.98}$$

Collecting the coefficients of like powers of e in the above equation results in

$$\begin{aligned}\dot{\Phi}_1(t, t_0) &= A_0\Phi_1(t, t_0) + A_1(t)\Phi_0(t, t_0) \\ \dot{\Phi}_2(t, t_0) &= A_0\Phi_2(t, t_0) + A_1(t)\Phi_1(t, t_0) + A_2(t)\Phi_0(t, t_0) \\ &\cdot \\ &\cdot \\ \dot{\Phi}_n(t, t_0) &= A_0\Phi_n(t, t_0) + A_1(t)\Phi_{n-1}(t, t_0) + \cdots + A_{n-1}(t)\Phi_1(t, t_0) \\ &\quad + A_n(t)\Phi_0(t, t_0)\end{aligned} \tag{5.99}$$

Melton presents expressions for the elements of Φ_1 and Φ_2 based on the following integrals:

$$\begin{aligned}\Phi_1(t, t_0) &= \int_{t_0}^{t} \Phi_0(t, s)A_1(s)\Phi_0(s, t_0)\mathrm{d}s \\ \Phi_2(t, t_0) &= \int_{t_0}^{t} \Phi_0(t, s)\left[A_1(s)\Phi_1(s, t_0) + A_2(s)\Phi_0(s, t_0)\right]\mathrm{d}s \\ &\cdot \\ &\cdot \\ \Phi_n(t, t_0) &= \int_{t_0}^{t} \Phi_0(t, s)\left[A_1(s)\Phi_{n-1}(s, t_0) + \cdots A_n(s, t_0)\Phi_0(s, t_0)\right]\mathrm{d}s\end{aligned} \tag{5.100}$$

Melton's solution shows the presence of secular terms for the in-plane motion variables. Secular terms appear in the along-track solution since the periods of the two satellites are, in general, not the same. However, the appearance of secular terms in the radial direction is an artifact of the series approximation utilized. Melton presents numerical results for eccentricities in the range $0 \leq e \leq 0.3$. These results clearly show the successive improvements achieved due to the first and second-order terms in the STM.

5.6.2 Lawden and Tschauner–Hempel Equations

Relative motion equations with true anomaly as the independent variable were derived in Eqs. (4.27)–(4.29). These equations have an interesting history. Lawden [110], during his studies on optimal orbit transfers, developed a set

of equations for the so-called *primer vector*, which can be used to describe perturbed motion with respect to elliptic orbits. Later, DeVries [111] and Tschauner and Hempel (TH) [102], independently arrived at the very same equations, while working respectively, on the problems of relative motion of particles and terminal rendezvous of spacecraft. Lawden was able to obtain a closed-form solution to his equations as well, involving an integral that has received considerable attention from subsequent researchers, most notably Carter [112]. The equations presented in this section are referred to as the *Tschauner–Hempel equations*:

$$\bar{x}'' = \frac{3}{k}\bar{x} + 2\bar{y}' \tag{5.101a}$$

$$\bar{y}'' = -2\bar{x}' \tag{5.101b}$$

$$\bar{z}'' = -\bar{z}' \tag{5.101c}$$

where $(\cdot)'$ and $(\cdot)''$ indicate, respectively, the first and second derivatives with respect to f, the true anomaly and $k = 1 + e\cos f$.

As can be seen from the above equations, the in-plane and out-of-plane equations are decoupled from each other. Equation (5.101b) can be integrated once to produce $\bar{y}'$, which, when substituted into Eq. (5.101a), gives

$$\bar{x}'' + \left[4 - \frac{3}{k}\right]\bar{x} = 2d \tag{5.102}$$

where d is a constant of integration. The solution to $\bar{x}$ enables one to obtain $\bar{y}$. Since Eq. (5.101c) describes a simple harmonic motion, its solution can be easily obtained. The solution to Eq. (5.102) developed by Lawden and its subsequent modifications by Carter [112] and Yamanaka and Ankersen [113] for the derivation of the STM are presented next.

5.6.3 Carter's STM

Two linearly-independent solutions to the homogeneous form of Eq. (5.102) (with $d = 0$), obtained by Lawden are

$$\bar{x}_1 = k\sin f \tag{5.103}$$

and

$$\bar{x}_2 = \bar{x}_1 \int \frac{1}{[k(f)\sin f]^2} df \tag{5.104}$$

Carter noted that the above integral is singular when f is a multiple of π. He eliminated this singularity by employing an alternate integral and provided a modified solution as shown below:

$$\bar{x}_2 = 2e\bar{x}_1 K_1(f) - \frac{\cos f}{k} \tag{5.105}$$

where

$$K_1(f) = \int \frac{\cos f}{k(f)^3} df \tag{5.106}$$

The above integral has a closed-form solution in terms of the eccentric anomaly [112]:

$$K_1(f) = (1-e^2)^{-5/2}\left[-\frac{3e}{2}E + (1+e^2)\sin E - \frac{e}{4}\sin 2E\right] \tag{5.107}$$

Carter's complete solution of Eq. (5.102) is

$$\bar{x} = c_1\bar{x}_1 + c_2\bar{x}_2 + c_3\bar{x}_3 \tag{5.108}$$

where

$$\bar{x}_3 = -2k\sin f K_1(f) - \cos^2 f/k - \cos^2 f \tag{5.109}$$

and $c_{1:3}$ are constants of integration. In particular, $c_3 = -d$, the constant appearing in the r.h.s. of Eq. (5.102).

Analytical solutions to the remaining variables can be written as

$$\begin{aligned} \bar{y} &= -2c_1 S(\bar{x}_1) - 2c_2 S(\bar{x}_2) - c_3 S(2\bar{x}_3 + 1) + c_4 \\ \bar{z} &= c_5\cos f + c_6 \sin f \end{aligned} \tag{5.110}$$

where $c_{4:6}$ are additional constants of integration and $S(.)$ represents integration w.r.t. f.

During the process of developing his STM, Carter encountered another singularity, associated with a term involving $K_1(f)/e$, which he eliminated using a modification to Eq. (5.105) as follows:

$$\bar{x}_2 = 2e\bar{x}_1\left[\frac{\sin f}{k^3} - 3eK_2(f)\right] - \frac{\cos f}{k} \tag{5.111}$$

where

$$K_2(f) = \int \frac{\sin^2 f}{k(f)^4} df \tag{5.112}$$

The resulting modified particular integral of Eq. (5.102) is

$$\bar{x}_3 = \left[6e\bar{x}_1 K_2(f) - 2\frac{\sin^2 f}{k^2} - \frac{\cos^2 f}{k} - \cos^2 f\right] \tag{5.113}$$

Carter constructed his STM by using the three fundamental solutions given by Eqs. (5.103), (5.111), and (5.113). The integral in Eq. (5.112) can also be

evaluated in closed-form, in terms of the eccentric anomaly:

$$K_2(f) = (1-e^2)^{-5/2}\left[\frac{1}{2}E - \frac{1}{4}\sin 2E - \frac{e}{3}\sin^3 E\right] \tag{5.114}$$

Note that the following ordering of the state variables is used in the presentation of Carter's STM: $\bar{\mathbf{x}} = \left[\bar{x}, \bar{x}', y, \bar{y}', z, \bar{z}'\right]^T$. The first step towards the derivation of the STM is to write the relationship between the state vector and the six constants of integration, $\mathbf{c} = [c_1, c_2, c_3, c_4, c_5, c_6]^T$:

$$\bar{\mathbf{x}} = \phi(f)\mathbf{c} \tag{5.115}$$

The constants can be conveniently evaluated at the initial true anomaly as

$$\mathbf{c} = \phi^{-1}(f(0))\mathbf{x}(f(0)) \tag{5.116}$$

Based on Eqs. (5.115) and (5.116), the STM can be written as

$$\Phi = \phi(f)\phi^{-1}(f(0)) \tag{5.117}$$

where

$$\phi(f) = \begin{bmatrix} \bar{x}_1 & \bar{x}_2 & \bar{x}_3 & 0 & 0 & 0 \\ \bar{x}_1' & \bar{x}_2' & \bar{x}_3' & 0 & 0 & 0 \\ -2S(\bar{x}_1) & -2S(\bar{x}_2) & -S(2\bar{x}_3+1) & -1 & 0 & 0 \\ -2\bar{x}_1 & -2\bar{x}_2 & -(2\bar{x}_3+1) & 0 & 0 & 0 \\ 0 & 0 & 0 & 0 & \cos f & \sin f \\ 0 & 0 & 0 & 0 & -\sin f & \cos f \end{bmatrix} \tag{5.118}$$

and

$$\phi^{-1}(f) = \begin{bmatrix} 4S(\bar{x}_2)+\bar{x}_2' & -\bar{x}_2 & 0 & 2S(\bar{x}_2) & 0 & 0 \\ -(4S(\bar{x}_1)+\bar{x}_1') & \bar{x}_1 & 0 & -2S(\bar{x}_1) & 0 & 0 \\ -2 & 0 & 0 & -1 & 0 & 0 \\ 2S(2\bar{x}_3+1)+\bar{x}_3' & -\bar{x}_3 & -1 & S(2\bar{x}_3+1) & 0 & 0 \\ 0 & 0 & 0 & 0 & \cos f & -\sin f \\ 0 & 0 & 0 & 0 & \sin f & \cos f \end{bmatrix} \tag{5.119}$$

where

$$\begin{aligned} S(\bar{x}_1) &= -\cos f\left[1 + \left(\frac{e}{2}\right)\cos f\right] \\ S(\bar{x}_2) &= 3ek^2K_2(f) - \frac{\sin f}{k} \\ S(2\bar{x}_3+1) &= -6k^2K_2(f) - \frac{2+k}{2k}\sin 2f \end{aligned} \tag{5.120}$$

5.6.4 Yamanaka and Ankersen's STM

Yamanaka and Ankerson (YA) [113] proposed a new form for the solution to the homogeneous version of Eq. (5.102) by noting the following identity:

$$I = \int_{f(0)}^{f} \frac{1}{k(f)^2} \mathrm{d}f = \frac{\mu^2}{h^3}(t - t_0) \tag{5.121}$$

Starting with $\bar{x}_1$, the fundamental solution of Lawden, they obtained a second independent solution as shown below:

$$\bar{x}_2 = 3e^2 I \bar{x}_1 + k\cos f - 2e \tag{5.122}$$

Based on the two linearly independent solutions given above, a particular solution to Eq. (5.102) can be written as follows:

$$\bar{x}_3 = (d/e)k\cos f \tag{5.123}$$

The singularity at $e = 0$ in $\bar{x}_3$ is eliminated when the complete solution is assembled:

$$\bar{x} = c_1 k\sin f + c_2 k\cos f + c_3(2 - 3ekI\sin f) \tag{5.124a}$$

$$\bar{y} = c_4 + c_1(1 + 1/k)\cos f - c_2(1 + 1/k)\sin f - 3c_3 k^2 I \tag{5.124b}$$

$$\bar{z} = c_5\cos f + c_6\sin f \tag{5.124c}$$

where $c_{1:6}$ are integration constants. The previously described procedure can be used to obtain the STM by eliminating the integration constants. As before, the state vector is defined as $\bar{\mathbf{x}} = \left[\bar{x}, \bar{x}', y, \bar{y}', z, \bar{z}'\right]^T$. The complete solution to Eq. (5.101) is

$$\bar{\mathbf{x}}(t) = \phi(f)\phi^{-1}(f(0))\bar{\mathbf{x}}(t_0) \tag{5.125}$$

where

$$\phi(f) = \begin{bmatrix} s & c & 2 - 3esI & 0 & 0 & 0 \\ s' & c' & -3e\left(s'I + \dfrac{s}{k^2}\right) & 0 & 0 & 0 \\ c\left(1 + \dfrac{1}{k}\right) & -s\left(1 + \dfrac{1}{k}\right) & -3k^2 I & 1 & 0 & 0 \\ -2s & e - 2c & -3(1 - 2esI) & 0 & 0 & 0 \\ 0 & 0 & 0 & 0 & \cos f & \sin f \\ 0 & 0 & 0 & 0 & -\sin f & \cos f \end{bmatrix} \tag{5.126}$$

with $c = k\cos f$ and $s = k\sin f$.

Note that the ordering of the state variables in this section is different from that used by Yamanaka and Ankersen in Ref. [113]. The explicit inverse of $\phi(f)$

evaluated at $f = f(0)$, which will prove useful later, has also been provided:

$$\phi^{-1}(f(0)) = \frac{1}{\eta^2} \times \begin{bmatrix} -3s\dfrac{k+e^2}{k^2} & c-2e & 0 & -s\dfrac{k+1}{k} & 0 & 0 \\ -3\left(e+\dfrac{c}{k}\right) & -s & 0 & -\left(c\dfrac{k+1}{k}+e\right) & 0 & 0 \\ 3k-\eta^2 & es & 0 & k^2 & 0 & 0 \\ -3es\dfrac{k+1}{k^2} & -2+ec & \eta^2 & -es\dfrac{k+1}{k} & 0 & 0 \\ 0 & 0 & 0 & 0 & \eta^2\cos f & -\eta^2\sin f \\ 0 & 0 & 0 & 0 & \eta^2\sin f & \eta^2\cos f \end{bmatrix} \tag{5.127}$$

where $\eta = \sqrt{1-e^2}$. The YA STM is very compact and simple to program.

5.6.5 Broucke's STM

Unlike the developments of Carter and Yamanaka and Ankersen, who used true anomaly as the independent variable to construct an analytical solution to the relative motion equations, Broucke [114] presents a form of the STM by using the analytical solution to the two-body problem. A brief treatment of Broucke's development of the fundamental matrix for the in-plane motion is presented here. The STM for the out-of-plane motion, as shown before, is very simple to write. Broucke's elegant approach to determining independent solutions for relative motion is based on expressing the variations of the chief's radius and velocity with respect to the four orbital elements $\mathbf{\text{œ}} = \{a \;\; e \;\; M_0 \;\; \omega\}$, along the radial and transverse directions:

$$x = \sum_{j=1}^{4} \frac{\partial r}{\partial \text{œ}_j}\delta\text{œ}_j \tag{5.128a}$$

$$y = \sum_{j=1}^{4} r\frac{\partial \theta}{\partial \text{œ}_j}\delta\text{œ}_j \tag{5.128b}$$

$$\dot{x} = \sum_{j=1}^{4} \frac{\partial \dot{r}}{\partial \text{œ}_j}\delta\text{œ}_j \tag{5.128c}$$

$$\dot{y} = \sum_{j=1}^{4} \left(\dot{r}\frac{\partial \theta}{\partial \text{œ}_j} + r\frac{\partial \dot{\theta}}{\partial \text{œ}_j}\right)\delta\text{œ}_j \tag{5.128d}$$

where $\delta\text{œ}_j$ represents a small change in the j^{th} element of $\mathbf{\text{œ}}$. Since r and θ depend on $\mathbf{\text{œ}}$, the variations due to these four orbital elements are required for the construction of the fundamental matrix, ϕ. The four columns of the

in-plane fundamental matrix are populated with the four linearly-independent solutions of x, y, $\dot{x}$, and $\dot{y}$ obtained from Eqs. (5.128). For example, the vector corresponding to the variations due to ω is

$$\phi(:,4) = \begin{bmatrix} 0 & r & 0 & \dot{r} \end{bmatrix}^T \tag{5.129}$$

A modification of the above scheme is required to eliminate the singularity in the fundamental matrix $e = 0$, since the columns generated by M_0 and ω are the same for $e = 0$. Hence, the column generated by the variations due to M_0 is replaced by the following linear combination to produce the desired fundamental matrix:

$$\begin{aligned} \phi(:,3) = \frac{\eta}{aen} &\begin{bmatrix} \dfrac{\partial r}{\partial M_0} & r\dfrac{\partial \theta}{\partial M_0} & \dfrac{\partial \dot{r}}{\partial M_0} & \dot{r}\dfrac{\partial \theta}{\partial M_0} + r\dfrac{\partial \dot{\theta}}{\partial M_0} \end{bmatrix}^T \\ -\frac{1}{ep} &\begin{bmatrix} \dfrac{\partial r}{\partial \omega} & r\dfrac{\partial \theta}{\partial \omega} & \dfrac{\partial \dot{r}}{\partial \omega} & \dot{r}\dfrac{\partial \theta}{\partial \omega} + r\dfrac{\partial \dot{\theta}}{\partial \omega} \end{bmatrix}^T \end{aligned} \tag{5.130}$$

The details of the elements of ϕ and ϕ^{-1} can be found in Ref. [114]. The final step of the calculation of the STM is given by Eq. (5.125). Note that Kepler's equation has to be solved at each time step of propagation with the Broucke STM.

5.6.6 STM of Lee, Cochran, and Jo

Lee, Cochran, and Jo (LCJ) [115] exploit the analytical solution to the two-body problem presented by Battin [33]. They use the following definition of the state vector in their work: $\mathbf{x} = [x, y, z, \dot{x}, \dot{y}, \dot{z}]^T$. The state vector at time t can be written as

$$\mathbf{x} = D(t) \begin{bmatrix} \delta r & \delta\theta & \delta\dot{r} & \delta\dot{\theta} & \delta i & \delta\Omega \end{bmatrix}^T \tag{5.131}$$

where

$$D(t) = \begin{bmatrix} 1 & 0 & 0 & 0 & 0 & 0 \\ 0 & r & 0 & 0 & 0 & r\cos i \\ 0 & 0 & 0 & 0 & r\sin\theta & -r\sin i\cos\theta \\ 0 & 0 & 1 & 0 & 0 & 0 \\ 0 & \dot{r} & 0 & r & 0 & \dot{r}\cos i \\ 0 & 0 & 0 & 0 & \dfrac{\mathrm{d}}{\mathrm{d}t}(r\sin\theta) & -\dfrac{\mathrm{d}}{\mathrm{d}t}(r\cos\theta)\sin i \end{bmatrix} \tag{5.132}$$

Next, they write

$$\begin{bmatrix} \delta r & \delta\theta & \delta\dot{r} & \delta\dot{\theta} & \delta i & \delta\Omega \end{bmatrix}^T = B(t,t_0) \begin{bmatrix} \delta r_0 & \delta\theta_0 & \delta\dot{r}_0 & \delta\dot{\theta}_0 & \delta i & \delta\Omega \end{bmatrix}^T \tag{5.133}$$

where

$$B(t,t_0)=\begin{bmatrix}\frac{\partial r(t)}{\partial r_0} & \frac{\partial r(t)}{\partial \theta_0} & \frac{\partial r(t)}{\partial \dot{r}_0} & \frac{\partial r(t)}{\partial \dot{\theta}_0} & 0 & 0\\ \frac{\partial \theta(t)}{\partial r_0} & \frac{\partial \theta(t)}{\partial \theta_0} & \frac{\partial \theta(t)}{\partial \dot{r}_0} & \frac{\partial \theta(t)}{\partial \dot{\theta}_0} & 0 & 0\\ \frac{\partial \dot{r}(t)}{\partial r_0} & \frac{\partial \dot{r}(t)}{\partial \theta_0} & \frac{\partial \dot{r}(t)}{\partial \dot{r}_0} & \frac{\partial \dot{r}(t)}{\partial \dot{\theta}_0} & 0 & 0\\ \frac{\partial \dot{\theta}(t)}{\partial r_0} & \frac{\partial \dot{\theta}(t)}{\partial \theta_0} & \frac{\partial \dot{\theta}(t)}{\partial \dot{r}_0} & \frac{\partial \dot{\theta}(t)}{\partial \dot{\theta}_0} & 0 & 0\\ 0 & 0 & 0 & 0 & 1 & 0\\ 0 & 0 & 0 & 0 & 0 & 1\end{bmatrix} \tag{5.134}$$

The elements of the sensitivity matrix, $B(t,t_0)$ have been developed in Ref. [115]. Equations (5.131) and (5.133) can be combined to arrive at the STM in the following form:

$$\Phi(t,t_0)=D(t)BD^{-1}(t_0) \tag{5.135}$$

Even though the nature of the LCJ STM appears to be time-explicit, Kepler's equation has to be solved at each time step.

5.6.7 STM of Nazarenko

An alternative approach, utilizing the two-body STM expressed in the chief-fixed rotating frame (the LVLH frame, $\mathscr{L}$), is presented by Nazarenko [116]. Recall that the STM for the two-body problem [33] is most commonly expressed in the inertial coordinate system. This STM can also be used for the propagation of relative motion if the relative state vector is expressed in the inertial reference frame. In this section the form of the relative state vector in the $\mathscr{L}$ frame is as defined by Eq. (5.93).

The relative position and the relative absolute velocity vectors in the $\mathscr{L}$ frame can be transformed into the $\mathscr{I}$ frame state vector as given below:

$$[\mathbf{x}(t)]_{\mathscr{I}}=\begin{bmatrix}C^T(t) & 0_{3\times3}\\ 0_{3\times3} & C^T(t)\end{bmatrix}\begin{bmatrix}I_3 & 0_{3\times3}\\ \tilde{\omega}(t) & I_3\end{bmatrix}\mathbf{x}(t) \tag{5.136}$$

where $C\equiv T_{\mathscr{I}}^{\mathscr{L}}$ is the DCM transforming from the $\mathscr{I}$ to the $\mathscr{L}$ frame (cf. Eq. (4.100)) and $\tilde{\omega}$ is the angular velocity cross-product matrix, defined by the usual convention that for any vector $\mathbf{v}=[v_1,v_2,v_3]^T$,

$$\tilde{\mathbf{v}}=\begin{bmatrix}0 & -v_3 & v_2\\ v_3 & 0 & -v_1\\ -v_2 & v_1 & 0\end{bmatrix} \tag{5.137}$$

Denoting

$$L(t) = \begin{bmatrix} C^T(t) & 0_{3\times3} \\ 0_{3\times3} & C^T(t) \end{bmatrix} \begin{bmatrix} I_3 & 0_{3\times3} \\ \tilde{\omega}(t) & I_3 \end{bmatrix} \tag{5.138}$$

it can be shown that

$$L(t)\mathbf{x}(t) = \Phi_{2B_{\mathscr{J}}} L(0)\mathbf{x}(0) \tag{5.139}$$

where $\Phi_{2B_{\mathscr{J}}}$ is the two-body STM, which can be found in Battin [33] (pp. 457–467). We can also make use of the following useful results for computing $\tilde{\omega}(t)$ in Eq. (5.138):

$$\dot{C}(t) = -\tilde{\omega}(t)C(t) \tag{5.140a}$$

$$\tilde{\omega}(t) = -\dot{C}(t)C^T(t) \tag{5.140b}$$

The matrices $C(t)$ and $\dot{C}(t)$ can be easily obtained from the solution of the two-body problem. Based on the above developments, the propagation equation for relative motion is

$$\mathbf{x}(t) = L^{-1}(t)\Phi_{2B_{\mathscr{J}}} L(0)\mathbf{x}(0) \tag{5.141}$$

Hence, the required STM for relative motion can be obtained as

$$\Phi(t, 0) = L^{-1}(t)\Phi_{2B_{\mathscr{J}}} L(0) \tag{5.142}$$

Details of the elements of the STM can be obtained from Ref. [116].

5.6.8 Initial conditions to prevent secular drift

The CW and TH equations and their associated STMs provide convenient means for describing linearized relative motion. They can be used to determine initial conditions for establishing a formation such that secular drift is prevented. Even though they may not be accurate but for the smallest of formations, they still provide good estimates for the desired initial conditions.

As we have seen in Section 4.2, the exact condition for eliminating secular drift for unperturbed motion is to match the periods of the satellites. In other words, the satellites must all have the same semimajor axes. We have also seen in Section 5.1 that the CW equations provide a condition for zero secular drift:

$$\dot{y} + 2nx = 0 \tag{5.143}$$

which is an approximation to the zero differential semimajor axis condition, since the effects of eccentricity and nonlinearity are not accounted for.

An improvement to the above condition can be obtained from the TH equations, which account for the effects of eccentricity. Inalhan *et al.* [117] noted that the general solution of Carter, Eqs. (5.110), predominantly involves

periodic functions. Secular terms in the in-plane equations appear only through the term K_1, as can be seen from Eq. (5.107). Hence, periodic trajectories of the TH equations can be set up by choosing initial conditions consistent with $c_2 = 0$ in Eq. (5.108). In their derivation of a boundedness condition, Inalhan et al. focused on the establishment of the formation at perigee or apogee of the reference orbit. However, a general condition for linear boundedness can be obtained from Carter's STM, which involves the integral $K_2(f)$. It can be seen from Eqs. (5.108), (5.111), and (5.113) that $K_2(f)$ can be eliminated from the in-plane motion solutions if the following relationship is satisfied:

$$c_3 - ec_2 = 0 \tag{5.144}$$

The coefficients c_2 and c_3 can be obtained from Eqs. (5.116) and (5.119) as

$$\begin{aligned} c_2 &= -\left[4S(\bar{x}_1) + \bar{x}_1'\right]\bar{x}(f(0)) + \bar{x}_1\bar{x}'(f(0)) - 2S(\bar{x}_1)\bar{y}'(f(0)) \\ c_3 &= -\left[2\bar{x}(f(0)) + \bar{y}'(f(0))\right] \end{aligned} \tag{5.145}$$

Substitution of Eqs. (5.145) and the first of Eq. (5.120) into Eq. (5.144) results in the following condition for boundedness:

$$\begin{aligned} &k^2(f(0))\bar{y}'(f(0)) + ek(f(0))\sin f(0)\bar{x}'(f(0)) \\ &\quad + \left[2 + 3e\cos f(0) + e^2\right]\bar{x}(f(0)) = 0 \end{aligned} \tag{5.146}$$

The same result can also be obtained from the YA STM by setting $c_3 = 0$ in Eq. (5.124), as shown by Sengupta and Vadali [1]. Jiang *et al.* also obtain the same condition by expanding the differential semimajor axis in terms of the relative motion variables.

Equation (5.146) can also be written by using the unscaled motion variables:

$$\begin{aligned} &k(f(0))y'(f(0)) + e\sin f(0)\left[x'(f(0)) - y(f(0))\right] \\ &\quad + [2 + e\cos f(0)]\,x(f(0)) = 0 \end{aligned} \tag{5.147}$$

and with time as the independent variable as well:

$$\begin{aligned} &k(f(0))\left[\dot{y}(t_0) + \dot{f}(0)x(t_0)\right] + e\sin f(0)\left[\dot{x}(t_0) - \dot{f}(0)y(t_0)\right] \\ &\quad + \dot{f}(0)x(t_0) = 0 \end{aligned} \tag{5.148}$$

where

$$\dot{f}(0) = \sqrt{\frac{\mu}{p^3}}k(f(0))^2 \tag{5.149}$$

The linear boundedness condition at any epoch is a function of the true anomaly, which can be found from Kepler's equation. It can be enforced in several ways, with a given relative position, since it involves both the radial and along-track relative velocities. However, satisfaction of Eq. (5.146) does

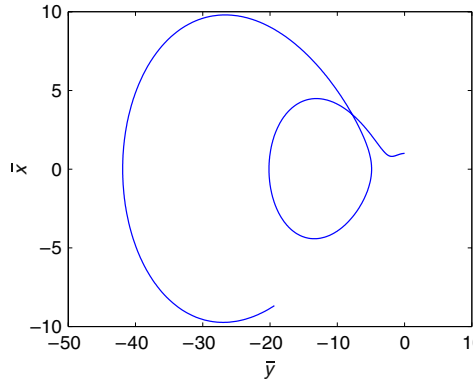

FIGURE 5.11 In-plane motion obtained using the YA STM.

not guarantee that the relative orbit will remain absolutely bounded, since the constraint is only a first-order approximation to $\delta a = 0$.

The use of the STM and the linear boundedness condition are demonstrated via a numerical example.

Example 5.5. *Assume that* $e = 0.5$ *and* $f(0) = \pi/2$. *Let the initial state of the relative motion be*

$$\left[\bar{x}, \bar{x}', y, \bar{y}'\right]^T = [\sin f(0), \cos f(0), 2\cos f(0), -2\sin f(0)]^T \quad (5.150)$$

A single-impulse maneuver is to be performed to establish periodic relative motion and center the relative orbit in the along-track direction. Obtain an estimate of the required impulse magnitude and the associated true anomaly of the chief at which the impulse should be performed.

First, the in-plane relative motion over a period of two orbits of the chief, propagated via the YA STM, is shown in Fig. 5.11. The solution obtained from numerical integration of Eqs. (5.101) is virtually indistinguishable from the STM result. It is observed that the motion is not periodic.

Next, an optimization problem is formulated to minimize the velocity correction required to satisfy Eq. (5.148). The velocity correction is sought as a function of f. Hence, the problem can be stated as

$$\begin{aligned}
&\text{minimize } k^2\{[(\bar{x}')^+ - (\bar{x}')^-]^2 + [(\bar{y}')^+ - (\bar{y}')^-]^2\} \\
&\text{s. t.} \\
&k^2(f)\bar{y}'(f) + ek(f)\sin f\bar{x}'(f) + \left[2 + 3e\cos f + e^2\right]\bar{x}(f) = 0
\end{aligned}$$

where $(\cdot)^-$ and $(\cdot)^+$ are respectively, quantities before and after impulse application.

The minimum cost, plotted as a function of f, is shown in Fig. 5.12. As can be seen, the cost is lowest at f values corresponding to multiples of 2π. Figure 5.13 shows the plots of the radial and transverse components of

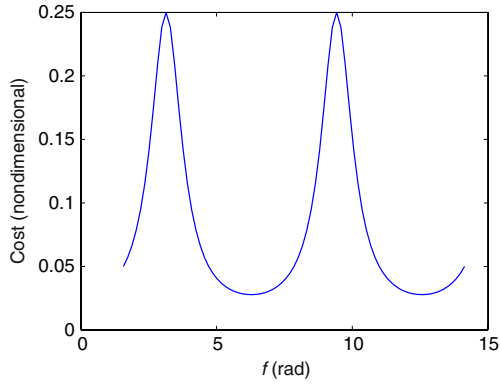

FIGURE 5.12 Cost as a function of f.

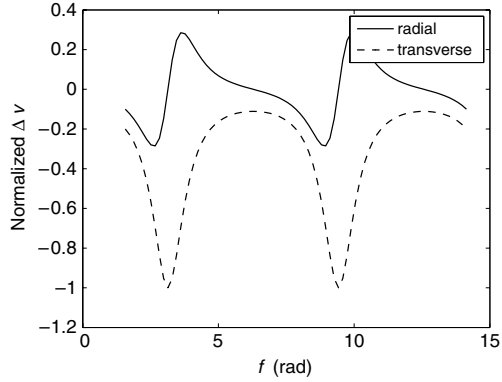

FIGURE 5.13 Normalized radial and transverse velocity increments.

the normalized Δv. Two important observations are: (i) the radial velocity correction is zero when f corresponds to either the periapsis or apoapsis locations; and (ii) the magnitude of the transverse component of the velocity correction has a local minimum at periapsis. These results can also be deduced from Eq. (5.146). It can be seen that when k^2 is at its extremum, $k \sin f = 0$, since $\frac{\mathrm{d}}{\mathrm{d}f} k^2 = 2ke \sin f$. Figure 5.14 shows the result of applying the velocity correction at $f = 2\pi$. The small circle in this figure indicates the location of the maneuver. The normalized, purely transverse velocity correction required is -0.11 units.

There remains the matter of centering the relative orbit with respect to the chief. One of the ways to accomplish this additional objective is to select the initial conditions such that $c_4 = 0$, in either Eq. (5.110) or Eq. (5.124). We see from Eqs. (5.116) and (5.127) that the above condition results in

$$e(k+1)\sin f\,\bar{y}'(f) + [2 - ek\cos f]\,\bar{x}'(f) + 3e\frac{k+1}{k}\sin f\,\bar{x}(f) - \eta^2\bar{y}(f) = 0 \tag{5.151}$$

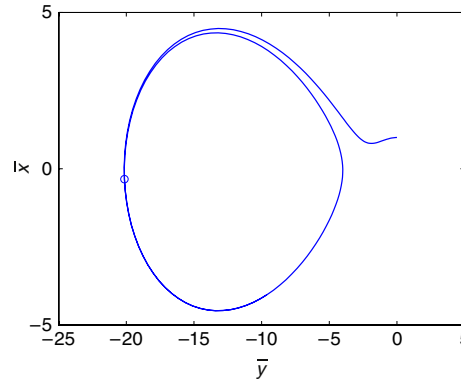

FIGURE 5.14 Result of the orbit establishment maneuver.

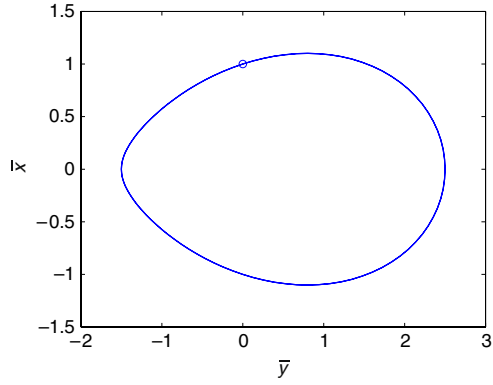

FIGURE 5.15 Single-impulse orbit establishment using two constraints.

Since Eqs. (5.146) and (5.151) represent two constraints involving the two velocity components, except for the choice of the true anomaly, there is no more room for optimization when a single impulse is used. For the initial conditions considered previously, the least cost is obtained when $f = \pi/2$ with a single radial impulse of -0.5 units. The resulting orbit is shown in Fig. 5.15. The small circle in this figure locates the point of application of the impulse.

A linear programming approach for minimum-fuel formation initialization and the analysis of the errors associated with neglecting eccentricity of the reference orbit can be found in Ref. [117]. Several other options of bias removal have been treated in Ref. [1].

5.7 PERIODIC SOLUTIONS TO THE TH EQUATIONS

Sengupta et al. [1] have estimated the relative motion drift rates for elliptic reference orbits due to semimajor axis mismatch by using Eqs. (5.124). By evaluating the expressions (5.124) at the beginning and at the end of an orbit of

the chief, it can be shown that

$$\bar{x}_{\text{drift}} = \bar{x}(f(0)+2\pi) - \bar{x}(f(0)) = -\frac{6k(f(0))\pi c_3}{\eta^3} e \sin f(0)$$
$$\bar{y}_{\text{drift}} = \bar{y}(f(0)+2\pi) - \bar{y}(f(0)) = -\frac{6k^2\pi c_3}{\eta^3} \tag{5.152}$$

where c_3 is the constant appearing in the development of the YA STM and it can be obtained from the third row of Eq. (5.127) as

$$\eta^2 c_3 = (3k(f(0)) - \eta^2)\bar{x}(f(0)) + ek(f(0))\sin(f(0))\bar{x}'(f(0)) + k(f(0))^2\bar{y}'(f(0)) \tag{5.153}$$

As noted in Section 5.4, c_3 is also related to the dimensional δa through

$$\frac{\delta a}{a} = 2c_3 \tag{5.154}$$

It has been shown in Ref. [1], based on Eqs. (5.152), that the radius of the in-plane xy-projection of the relative orbit undergoes a per-orbit drift given by

$$\rho_{\text{drift}} = \left(x_{\text{drift}}^2 + y_{\text{drift}}^2\right)^{1/2} = \frac{3\pi}{\eta}\,\delta a[1+e^2+2e\cos f(0)]^{1/2} \tag{5.155}$$

Hence, ρ_{drift} is bounded by

$$3\pi\,\delta a\sqrt{\frac{1-e}{1+e}} \le \rho_{\text{drift}} \le 3\pi\,\delta a\sqrt{\frac{1+e}{1-e}} \tag{5.156}$$

If $c_3 = 0$, then the periodic solutions to the TH equations can be obtained as

$$\bar{x} = \frac{\rho_x}{p}\sin(f+\alpha_x)\,(1+e\cos f) \tag{5.157a}$$
$$\bar{y} = \frac{\rho_x}{p}\cos(f+\alpha_x)\,(2+e\cos f) + \frac{\rho_y}{p} \tag{5.157b}$$
$$\bar{z} = \frac{\rho_z}{p}\sin(f+\alpha_z) \tag{5.157c}$$

The periodic solutions to the TH equations can also be represented in dimensional form as

$$x = \rho_x \sin(f+\alpha_x) \tag{5.158a}$$
$$y = 2\rho_x\cos(f+\alpha_x)\frac{(1+(e/2)\cos f)}{(1+e\cos f)} + \frac{\rho_y}{(1+e\cos f)} \tag{5.158b}$$
$$z = \rho_z\frac{\sin(f+\alpha_z)}{(1+e\cos f)} \tag{5.158c}$$

Equations (5.158) show the presence of higher-order harmonics in the motion variables induced due to eccentricity. Fourier series representations of the motion variables with true anomaly and time as the independent variables are provided in Ref. [1]. Only the expressions for y are given here, in truncated forms, to show three different methods for correcting for the along-track bias present in the solution (5.158). The result with f as the independent variable is

$$y(f) = \frac{1}{\eta}\left[-\varepsilon\rho_x \cos\alpha_x + \rho_y\right] + (h.o.t) \tag{5.159}$$

where $\varepsilon = \sqrt{[(1-\eta)/(1+\eta)]}$ and we have, with time as the independent variable,

$$y(t) = \frac{1}{2\eta^2}\left[-e(3+2\eta^2)\rho_x \cos\alpha_x + (3-\eta^2)\rho_y\right] + (h.o.t) \tag{5.160}$$

Equation (5.159) shows that the bias term therein can be removed by enforcing the condition

$$\rho_y = \varepsilon\rho_x \cos\alpha_x \tag{5.161}$$

This correction, labeled *f-correction*, does not have any significance in the time domain. From Eq. (5.160), we get an alternate condition, labeled *t-correction*, for the elimination of the bias term which allows the deputy to spend equal time ahead and behind the chief:

$$\rho_y = [e(3+2\eta^2)/(3-\eta^2)]\rho_x \cos\alpha_x \tag{5.162}$$

A third condition can also be obtained by requiring symmetry of motion given by Eqs. (5.158) at $f = 0$ and $f = \pi$. This correction is termed the *amplitude correction*:

$$\rho_y = e\rho_x \cos\alpha_x \tag{5.163}$$

The results [1] of the application of the three corrections are shown in Fig. 5.16, for $e = 0.6$, $\rho_x = 1/2$ km, $\rho_z = 1$ km and $\alpha_x = \alpha_z = 0$. Of the three corrections, only Eq. (5.163) allows the motion to be symmetrically bounded with respect to the chief.

The modification or distortion of the ideal PCO of the CW equations due to the effect of eccentricity is illustrated in Fig. 5.17 for $2\rho_x = \rho_z = 1$ km and $\alpha_x = \alpha_z = 0$, for $e = 0.2$ and $e = 0.7$. In these figures, the dashed-dotted lines show the ideal PCOs. The application of Eq. (5.148) to determine the corrected $\dot{y}(0)$ provides bounded relative orbits, as shown by the dashed lines. The bias removal is achieved by applying Eq. (5.163), resulting in the solid lines. Note the drastic change produced by the bias correction for $e = 0.7$.

Thus, the relative orbits can be corrected for the effects of nonlinearity as well as eccentricity. Considering the effects of nonlinearity and eccentricity

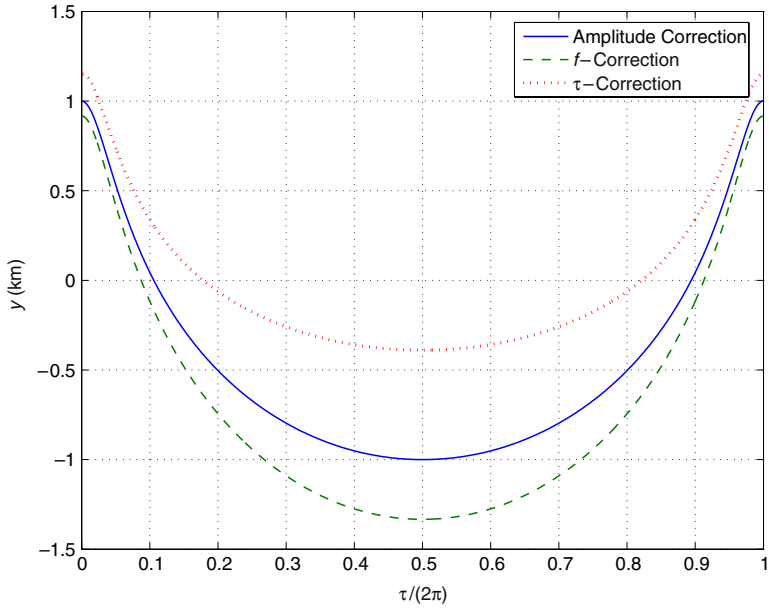

FIGURE 5.16 Effect of the three bias correction formulas, $e = 0.6$ (adapted from Ref. [1]).

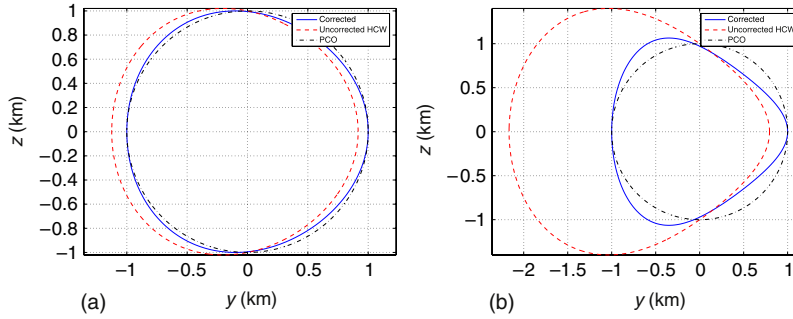

FIGURE 5.17 (a) Corrected PCO relative orbits, $e = 0.2$. (b) Corrected PCO relative orbits, $e = 0.7$ (adapted from Ref. [1]).

separately shows the connections between the CW relative orbit shape-size parameters and the along-track bias and drift rate. However, ultimately, it is the $\delta a = 0$ constraint that has to be satisfied for bounded unperturbed relative motion, and it can be satisfied in several different ways.

SUMMARY

In this chapter, we presented linear relative motion models for circular and elliptic reference orbits. The famous CW equations, which have been widely used for rendezvous and formation design and analysis, were introduced. We also

treated the relative motion problem using Lagrangian and Hamiltonian mechanics and derived the higher-order nonlinear versions of the CW equations. The perturbation solution to these equations presented us with a means to estimate the drift rate due to the nonlinear effects associated with a circular reference orbit. The advantages of writing the equations of motion in a curvilinear coordinate system for capturing some of the nonlinear effects were also demonstrated in this chapter. The treatment of the elliptic orbit case lead us to the Tschauner–Hempel equations and the various forms of the two-body STMs for the propagation of relative motion. We also presented a first-order boundedness condition for elliptic orbits and a method for the along-track bias removal to shape the relative orbit geometry.